IMA Journal of Applied Mathematics (2015) **80**, 1534–1568
doi:10.1093/imamat/hxv006
Advance Access publication on 8 May 2015

Spatial, temporal and spatiotemporal patterns of diffusive predator–prey models with mutual interference

Hong-Bo Shi
School of Mathematical Science, Huaiyin Normal University, Huaian, Jiangsu 223300, People's Republic of China

and

Shigui Ruan*
Department of Mathematics, University of Miami, Coral Gables, FL 33124-4250, USA
*Corresponding author: ruan@math.miami.edu

[Received on 27 January 2014; revised on 26 November 2014; accepted on 31 March 2015]

In this paper, the spatial, temporal and spatiotemporal dynamics of a reaction–diffusion predator–prey system with mutual interference described by the Crowley–Martin-type functional response, under homogeneous Neumann boundary conditions, are studied. Preliminary analysis on the local asymptotic stability and Hopf bifurcation of the spatially homogeneous model based on ordinary differential equations is presented. For the reaction–diffusion model, firstly the invariance, uniform persistence and global asymptotic stability of the coexistence equilibrium are discussed. Then it is shown that Turing (diffusion-driven) instability occurs, which induces spatial inhomogeneous patterns. Next it is proved that the model exhibits Hopf bifurcation which produces temporal inhomogeneous patterns. Furthermore, at the points where the Turing instability curve and Hopf bifurcation curve intersect, it is demonstrated that the model undergoes Turing–Hopf bifurcation and exhibits spatiotemporal patterns. Finally, the existence and non-existence of positive non-constant steady states of the reaction–diffusion model are established. Numerical simulations are presented to verify and illustrate the theoretical results.

Keywords: diffusive predator–prey model; mutual interference; Turing instability; Hopf bifurcation; Turing–Hopf bifurcation; positive non-constant steady states.

1. Introduction

A functional response of predators to their prey density refers to the change in the density of the prey attached per unit time per predator as the prey density changes. The most widely used functional response function, proposed by Holling (1965) and called Holling type II or Michaelis–Menten type, describes the average feeding rate of a predator when the predator spends some time searching for prey and some time processing the captured prey (that is, handling time, Cosner *et al.*, 1999) and takes the form

$$p(u) = \frac{mu}{1 + au}, \tag{1.1}$$

where u represents the density of the prey population, and the positive constants m (units: 1/times) and a (units: 1/prey) describe the effects of capture rate and handling time, respectively, on the feeding rate. Note that the Holling type II function is prey-dependent and is not affected by the abundance of the predator population (Jost, 2000).

The derivation of the Holling type II function (1.1) was based on the assumption that predators do not interference with one another's activities (Holling, 1965; Cosner *et al.*, 1999), so the only competition among predators occurs in the depletion of prey. To describe mutual interference among predators, Beddington (1975) and DeAngelis *et al.* (1975) proposed that individuals from a population of more than two predators not only allocate time in searching for and processing their prey but also take time in encountering with other predators. This results in the so-called Beddington–DeAngelis functional response (Cantrell & Cosner, 2001; Zhang *et al.*, 2012)

$$p(u,v)=\frac{mu}{1+au+bv}, \tag{1.2}$$

where v denotes the density of the predators and the parameter b (units: 1/predator) describes the magnitude of interference among predators. Note that when $b=0$, the Beddington–DeAngelis functional response reduces to the Holling type II function (1.1).

In the Beddington–DeAngelis functional response, interference and handling are assumed to be exclusive. Subsequently, Crowley & Martin (1989) assumed that interference among predators occurs no matter if a particular predator is searching for prey or handling prey and proposed a functional response of the form

$$p(u,v)=\frac{mu}{1+au+bv+abuv}=\frac{mu}{(1+au)(1+bv)}, \tag{1.3}$$

which is called the Crowley–Martin-type functional response in the literature (Skalski & Gilliam, 2001). It is assumed that the predator feeding rate decreases by higher predator density even when prey density is high, and therefore the effects of predator interference in the feeding rate remain important all the time whether an individual predator is handling or searching for a prey at a given time. Note that if $b=0$, then Crowley–Martin-type functional response (1.3) also reduces to Holling type II functional response (1.2).

Though the Crowley–Martin functional response is similar to the Beddington–DeAngelis functional response but it has an extra term $abuv$ in the denominator which may induce different dynamical properties. Moreover, in fitting different types of predator–prey data sets Skalski & Gilliam (2001) observed that the Beddington–DeAngelis functional response fits better for some data sets, while the Crowley–Martin functional response fits better for some others. Based on these observations, they suggested use of the Beddington–DeAngelis functional response when the predator feeding rate becomes independent of the predator density at high prey density and the Crowley–Martin functional response when the predator feeding rate is decreased by higher predator density even when the prey density is high.

In the monograph of May (1973), the following model was proposed (see also Tanner, 1975):

$$\begin{cases}\dfrac{\mathrm{d}u}{\mathrm{d}t}=ru\left(1-\dfrac{u}{K}\right)-\dfrac{muv}{1+au},\\[2ex] \dfrac{\mathrm{d}v}{\mathrm{d}t}=sv\left(1-\dfrac{v}{hu}\right),\end{cases} \tag{1.4}$$

where u and v represent prey and predator densities and r and s denote their intrinsic growth rates, respectively; K is the carrying capacity of the prey's environment, while the carrying capacity of the predator's environment, u/h, is a function on the prey population size (h is a measure of the food quality of the prey for conversion into predator growth depending on the density of the prey population). The saturating predator functional response is of Holling type II. The form of the predator equation in system (1.4) was first introduced by Leslie (1948). The term $(v/\gamma u)$ $(\gamma=h/s)$is called the Leslie–Gower term

(Leslie & Gower, 1960). The Leslie–Gower-type predator–prey model with Holling type II functional response is also called the Holling–Tanner model (May, 1973; Murray, 1989). Caughley (1976) used this system to model the biological control of the prickly-pear cactus by the moth *Cactoblastis cactorum*. Wollkind *et al.* (1988) employed this model to study the temperature-mediated stability of the predator–prey mite interaction between *Metaseiulus occidentalis* and the phytophagous spider mite *Tetranychus mcdanieli* on apple trees. Collings (1997) further suggested that the Holling type II functional response in system (1.4) can be replaced by other functions, such as the Holling types III and IV functions. Predator–prey models of Leslie–Gower type with generalized Holling type III and Holling type IV functions were studied by Hsu & Huang (1995), Huang *et al.* (2014) and Li & Xiao (2007), respectively. See also Freedman & Mathsen (1993).

Following Skalski & Gilliam (2001) and Collings (1997), when the predator feeding rate is decreased by higher predator density even when prey density is high, it is more reasonable to consider a Leslie–Gower-type predator–prey model with Crowley–Martin functional response describing the predator mutual interference, which takes the form

$$\begin{cases} \dfrac{\mathrm{d}u}{\mathrm{d}t} = ru\left(1-\dfrac{u}{K}\right) - \dfrac{muv}{(1+au)(1+bv)}, \\ \dfrac{\mathrm{d}v}{\mathrm{d}t} = sv\left(1-\dfrac{v}{hu}\right), \end{cases} \tag{1.5}$$

where the parameters r, K, a, b, h, m and s have the same meanings as introduced above.

On the other hand, in the evolutionary process of population species, individuals do not remain fixed in space and their spatial distributions change continuously due to the impact of many factors (environment, food supplies, season, etc.). Therefore, different spatial effects have been introduced into population models, such as diffusion and dispersal (Cantrell & Cosner, 2003). To study the spatiotemporal dynamics of the predator–prey model, we consider the following partial differential equation model under homogeneous Neumann boundary conditions

$$\begin{cases} \dfrac{\partial u}{\partial t} - d_1\Delta u = ru\left(1-\dfrac{u}{K}\right) - \dfrac{muv}{(1+au)(1+bv)}, \quad x\in\Omega,\ t>0, \\ \dfrac{\partial v}{\partial t} - d_2\Delta v = sv\left(1-\dfrac{v}{hu}\right), \quad x\in\Omega,\ t>0, \\ \dfrac{\partial u}{\partial \nu} = \dfrac{\partial v}{\partial \nu} = 0, \quad x\in\partial\Omega,\ t>0, \\ u(x,0)=u_0(x)\geqslant 0,\ v(x,0)=v_0(x)\geqslant 0, \quad x\in\Omega. \end{cases} \tag{1.6}$$

Here, $u(x,t)$ and $v(x,t)$ stand for the densities of the prey and predators at location $x\in\Omega$ and time t, respectively; $\Omega\subset R^N (N\leqslant 3)$ is a bounded domain with smooth boundary $\partial\Omega$; ν is the outward unit normal vector of the boundary $\partial\Omega$. The homogeneous Neumann boundary conditions indicate that the predator–prey system is self-contained with zero population flux across the boundary. The positive constants d_1 and d_2 are diffusion coefficients, and the initial data $u_0(x)$ and $v_0(x)$ are non-negative continuous functions.

Spatial, temporal and spatiotemporal patterns could occur in the reaction–diffusion model (1.6) via four possible mechanisms: Turing instability, Hopf bifurcation, Turing–Hopf bifurcation and positive non-constant steady states.

(a) *Spatial inhomogeneous patterns via Turing instability.* In his seminal work, Turing (1952) investigated reaction–diffusion equations of two chemicals and found that diffusion could destabilize an otherwise stable steady state. This mechanism leads to non-uniform spatial patterns which could then generate biological patterns by gene activation. This kind of instability is usually called *Turing instability* (Murray, 1989) or *diffusion-driven instability* (Okubo, 1980). Segel & Jackson (1972) was the first to show that Turing instability may occur in ecological systems; more precisely, they proved that the uniform steady state of a diffusive predator–prey model could be unstable if the predators exhibit self-limiting or intraspecific competition. See also Levin (1974) for a similar model and conclusion. Thus classical prey-dependent diffusive predator–prey models cannot give rise to spatial structures through diffusion-driven instability. Segel & Levin (1976) used a combination of successive approximation and multiple-time scale theory to develop the small amplitude non-linear theory for the diffusive predator–prey model considered in Segel & Jackson (1972), and showed that a new non-uniform steady state would be attained following destabilization of the spatially uniform steady state. Levin & Segel (1976) pointed out that Turing instabilities might explain the instance of spatial irregularity in the observed patchy distribution of plankton in the ocean. Wollkind *et al.* (1991) showed that Turing instability occurs in a diffusive Leslie–Gower-type predator–prey model with a Holling type II function or Holling–Tanner model, that is, the reaction–diffusion equation version of system (1.4). Thus, the self-limiting or intraspecific competition effect of the predators can be relaxed if the carrying capacity of predator's environment is described by a Leslie–Gower term. Alonson *et al.* (2002) demonstrated that predator-dependent diffusive predator–prey models, such as the diffusive predator–prey model with ratio-dependent functional response function, can also generate patchiness in a homogeneous environment via Turing instability. For reviews and related work on Turing instability and Turing pattern formation of reaction–diffusion systems from applied sciences, we refer the reader to Levin & Segel (1985), Malchow *et al.* (2008) and references cited therein.

(b) *Temporal periodic patterns via Hopf bifurcation*. The Hopf bifurcation theorem gives a set of sufficient conditions to ensure that an autonomous differential equation with a parameter exhibits non-trivial time-periodic solutions for certain values of the parameter. Ruan *et al.* (1998) studied Hopf bifurcation in a diffusive predator–prey model; see recent studies in Li *et al.* (2013) and Yi *et al.* (2009) on other predator–prey models. Thus, diffusive predator–prey models with suitable functional response can generate temporal periodic patterns via Hopf bifurcation.

(c) *Spatiotemporal patterns via Turing–Hopf bifurcation*. For a given reaction–diffusion system, when the Hopf bifurcation curve and Turing bifurcation curve intersect, at the codimension-2 bifurcation point a new bifurcation, called *Turing–Hopf bifurcation*, occurs and generates spatiotemporal patterns. The interaction of Turing and Hopf bifurcations in chemical and physical systems has been observed and analysed since the early 1990s (see Rovinsky & Menzinger, 1992; Meixner, 1997; Wit *et al.*, 1996). Recently, for a generalized predator–prey model on a spatial domain. Baurmanna *et al.* (2007) derived conditions for the existence of codimension-2 Turing–Hopf and codimension-3 Turing–Takens–Bogdanov bifurcation which give rise complex pattern formation processes.

(d) *Spatial patterns via positive non-constant steady states.* For reaction–diffusion systems, another possible mechanism that can produce spatial patterns is the existence of positive non-constant steady states. Du & Hsu (2004) considered a diffusive Leslie–Gower predator–prey model and showed that positive steady-state solutions with certain prescribed spatial patterns can be obtained if the coefficient functions are chosen suitably. Pang & Wang (2003) studied a diffusive Holling–Tanner predator–prey model and obtained the existence and non-existence of positive non-constant steady states. See also Ryu & Ahn (2005), Zhang *et al.* (2011) and the references cited therein.

The goal of this article is to show that the diffusive predator–prey model (1.6) exhibits various spatial, temporal and spatiotemporal patterns via the above-mentioned four mechanisms. For the sake of simplicity, by applying the following scaling:

$$rt \mapsto t,\ \frac{u}{K} \mapsto u,\ \frac{v}{Kh} \mapsto v,\ \frac{mKh}{r} \mapsto m,\ aK \mapsto a,\ bKh \mapsto b,\ \frac{s}{r} \mapsto s,\ \frac{d_1}{r_1} \mapsto d_1,\ \frac{d_2}{r_1} \mapsto d_2,$$

system (1.6) can be simplified as follows:

$$\begin{cases} \dfrac{\partial u}{\partial t} - d_1 \Delta u = u(1-u) - \dfrac{muv}{(1+au)(1+bv)}, & x \in \Omega,\ t > 0, \\ \dfrac{\partial v}{\partial t} - d_2 \Delta v = sv\left(1 - \dfrac{v}{u}\right), & x \in \Omega,\ t > 0, \\ \dfrac{\partial u}{\partial \nu} = \dfrac{\partial v}{\partial \nu} = 0, & x \in \partial\Omega,\ t > 0, \\ u(x,0) = u_0(x) \geqslant 0,\ v(x,0) = v_0(x) \geqslant 0, & x \in \Omega. \end{cases} \tag{1.7}$$

The rest of this paper is organized as follows. In Section 2, we investigate the asymptotical behaviour of the interior equilibrium and occurrence of Hopf bifurcation of the local system (the ODE model) of (1.7). In Section 3, we firstly discuss the invariance, uniform persistence and global asymptotic stability of the coexistence equilibrium for reaction–diffusion system (1.7). Then we consider the Turing (diffusion-driven) instability of the coexistence equilibrium for the reaction–diffusion system (1.7) when the spatial domain is a bounded interval, which will produce spatial inhomogeneous patterns. Thirdly, we study the existence and direction of Hopf bifurcation and the stability of the bifurcating periodic solution, which is a spatially homogeneous periodic solution of the reaction–diffusion system (1.7) and exhibits temporal periodic patterns. Next we investigate the interaction of the Turing instability and Hopf bifurcation, that is, the existence of Turing–Hopf bifurcation in the reaction–diffusion system (1.7) which will demonstrate spatiotemporal patterns. Numerical simulations are presented to verify the theoretical results. In Section 4, we establish the existence and non-existence of positive non-constant steady states of reaction–diffusion system (1.7). We end our study with some discussions in Section 5.

2. Stability and Hopf bifurcation of the local system

For the sake of completeness, we first consider the dynamics of the spatially homogeneous model of the diffusive predator–prey system (1.7), based on the following ordinary differential equations:

$$\begin{cases} \dfrac{\mathrm{d}u}{\mathrm{d}t} = u(1-u) - \dfrac{muv}{(1+au)(1+bv)}, \\ \dfrac{\mathrm{d}v}{\mathrm{d}t} = sv\left(1 - \dfrac{v}{u}\right). \end{cases} \tag{2.1}$$

We can see that system (2.1) has a boundary equilibrium point $\mathbf{e}_1 = (1,0)$. Since $u(t)$ and $v(t)$ represent population densities, we are interested in the existence of an interior equilibrium $\mathbf{e}^* = (u^*, v^*)$ (i.e. $u^* > 0$, $v^* > 0$), where u^* and v^* are positive solutions of the following algebraic equations:

$$1 - u^* - \frac{mv^*}{(1+au^*)(1+bv^*)} = 0 \quad \text{and} \quad \frac{v^*}{u^*} = 1.$$

Thus, system (2.1) has a unique positive equilibrium (u^*, v^*) if and only if the cubic equation

$$abu^3 + (a + b - ab)u^2 + (m + 1 - a - b)u - 1 = 0 \tag{2.2}$$

has a unique positive root. In fact, if $a + b \geqslant ab$, then (2.2) has a unique positive root u^*, by Cardan's formula, given by

$$u^* = \sqrt[3]{q + \sqrt{q^2 + (n - p^2)^3}} + \sqrt[3]{q - \sqrt{q^2 + (n - p^2)^3}} + p,$$

where

$$n = \frac{m + 1 - a - b}{3ab}, \quad p = \frac{ab - a - b}{3ab}, \quad q = p^3 + \frac{(a + b - ab)(m + 1 - a - b) + 3ab}{6a^2b^2}.$$

Note that (u^*, v^*) is also a constant steady-state solution of the diffusive system (1.7) under the Neumann boundary conditions. From the viewpoint of ecology, the asymptotic properties of the positive equilibrium are interesting and important.

A straight calculation yields that the Jacobian matrix of system (2.1) at (u^*, v^*) is

$$J := \begin{pmatrix} s_0 & \sigma \\ s & -s \end{pmatrix}, \tag{2.3}$$

where

$$s_0 = u^* \left(\frac{amu^*}{(1 + au^*)^2(1 + bu^*)} - 1 \right) \quad \text{and} \quad \sigma = -\frac{mu^*}{(1 + au^*)(1 + bu^*)^2}.$$

The characteristic polynomial is

$$P(\lambda) = \lambda^2 - \Theta\lambda + \Delta,$$

where $\Theta := s_0 - s$ and

$$\Delta := -s(s_0 + \sigma) = \frac{su^*[m + (1 + au^*)^2(1 + bu^*)^2 - abmu^{*2}]}{(1 + au^*)^2(1 + bu^*)^2}.$$

Thus, we have the following conclusions.

PROPOSITION 2.1 Assume that $a + b \geqslant ab$.

(i) If $s > s_0$ and

$$(\mathrm{H}_1) \quad m + (1 + au^*)^2(1 + bu^*)^2 > abmu^{*2},$$

then the positive equilibrium (u^*, v^*) is locally asymptotically stable.

(ii) If (H_1) and

$$(\mathrm{H}_2) \quad amu^* > (1 + au^*)^2(1 + bu^*)$$

are satisfied, then the positive equilibrium (u^*, v^*) is unstable when $s < s_0$.

(iii) If

$$(H_3) \quad m + (1 + au^*)^2(1 + bu^*)^2 < abmu^{*2},$$

then the positive equilibrium (u^*, v^*) is a saddle point.

REMARK 2.2 In case (i), s_0 is permitted to be positive or negative. If $s_0 < 0$, that is,

$$amu^* < (1 + au^*)^2(1 + bu^*), \tag{2.4}$$

then we have

$$abmu^{*2} < (1 + au^*)^2(1 + bu^*)bu^* < (1 + au^*)^2(1 + bu^*)^2 + m, \tag{2.5}$$

which indicates that (H_1) holds. For case (ii), s_0 must be positive. Moreover, we can see that conditions (H_1) and (H_2) can hold simultaneously. Furthermore, from (2.4), (2.5) and (H_3), we know that s_0 is positive in case (iii).

In the following, we analyse the existence of Hopf bifurcation at the interior equilibrium (u^*, v^*) by choosing s as the bifurcation parameter. In fact, s can be regarded as the intrinsic growth rate of predators and plays an important role in determining the stability of the interior equilibrium and the existence of Hopf bifurcation.

Assume that (H_1) and (H_2) hold, which guarantee that $s_0 > 0$ and $\Delta > 0$. Define $\rho = \sqrt{\Delta}$. We can see that the Jacobian matrix of system (2.1) has a pair of purely imaginary eigenvalues $\lambda = \pm i\rho$ when $s = s_0$. Therefore, according to Poincaré–Andronov–Hopf Bifurcation Theorem, system (2.1) has a small amplitude non-constant periodic solution bifurcated from the interior equilibrium (u^*, v^*) when r crosses through s_0 if the transversality condition is satisfied.

Let $\lambda(s) = \alpha(s) \pm i\beta(s)$ be a pair of complex roots of $P(\lambda) = 0$ when s is near s_0. Then we have $\alpha(s) = \frac{1}{2}(s_0 - s)$ and $\beta(s) = \frac{1}{2}\sqrt{-4s\sigma - (s_0 + s)^2}$. Hence, $\alpha(s_0) = 0$ and $\alpha'(s_0) = -\frac{1}{2} < 0$. This shows that the transversality condition holds. Thus (2.1) undergoes a Hopf bifurcation about (u^*, v^*) as s passes through the s_0.

To understand the detailed property of the Hopf bifurcation, we need a further analysis of the normal form. We translate the interior equilibrium (u^*, v^*) to the origin by the transformation $\tilde{u} = u - u^*$, $\tilde{v} = v - v^*$. For the sake of convenience, we still denote $\tilde{u}$ and $\tilde{v}$ by u and v, respectively. Thus, the local system (2.1) is transformed into

$$\begin{cases} \dfrac{du}{dt} = (u + u^*) - (u + u^*)^2 - \dfrac{m(u + u^*)(v + v^*)}{(1 + a(u + u^*))(1 + b(v + v^*))}, \\ \dfrac{dv}{dt} = s(v + v^*)\left(1 - \dfrac{v + v^*}{u + u^*}\right). \end{cases} \tag{2.6}$$

Rewrite system (2.6) as

$$\begin{pmatrix} \dfrac{du}{dt} \\ \dfrac{dv}{dt} \end{pmatrix} = J \begin{pmatrix} u \\ v \end{pmatrix} + \begin{pmatrix} f(u, v, s) \\ g(u, v, s) \end{pmatrix}, \tag{2.7}$$

where

$$f(u,v,s) = a_1u^2 + a_2uv + a_3u^3 + a_4u^2v + \cdots,$$
$$g(u,v,s) = b_1u^2 + b_2uv + b_3v^2 + b_4u^3 + b_5u^2v + b_6uv^2 + \cdots$$

and

$$a_1 = -1 + \frac{amu^*}{(1+au^*)^3(1+bu^*)}, \quad a_2 = -\frac{m}{(1+au^*)^2(1+bu^*)^2},$$
$$a_3 = -\frac{a^2mu^*}{(1+au^*)^4(1+bu^*)}, \quad a_4 = \frac{am}{(1+au^*)^3(1+bu^*)^2},$$
$$b_1 = -\frac{s}{u^*}, \quad b_2 = \frac{2s}{u^*}, \quad b_3 = -\frac{s}{u^*}, \quad b_4 = \frac{s}{u^{*2}}, \quad b_5 = -\frac{2s}{u^{*2}}, \quad b_6 = \frac{s}{u^{*2}}.$$

Set the matrix

$$P := \begin{pmatrix} N & 1 \\ M & 0 \end{pmatrix},$$

where $M = -s/\beta$ and $N = -(s_0 + s)/2\beta$. It is easy to obtain that

$$P^{-1}JP = \Phi(s) := \begin{pmatrix} \alpha(s) & -\beta(s) \\ \beta(s) & \alpha(s) \end{pmatrix}.$$

When $s = s_0$, we have

$$M_0 := M|_{s=s_0} = -\frac{s_0}{\beta_0}, \quad N_0 := N|_{s=s_0} = -\frac{s_0}{\beta_0}, \quad \beta_0 := \beta(s_0) = \sqrt{-s_0(s_0+\sigma)}. \tag{2.8}$$

By the transformation $(u,v)^\top = P(x,y)^\top$, system (2.7) becomes

$$\begin{pmatrix} \frac{\mathrm{d}x}{\mathrm{d}t} \\ \frac{\mathrm{d}y}{\mathrm{d}t} \end{pmatrix} = \Phi(s) \begin{pmatrix} x \\ y \end{pmatrix} + \begin{pmatrix} f^1(x,y,s) \\ g^1(x,y,s) \end{pmatrix}, \tag{2.9}$$

and

$$\begin{aligned} f^1(x,y,s) &= \frac{1}{M} g(Nx+y, Mx, s) \\ &= \left(\frac{N^2}{M}b_1 + Nb_2 + Mb_3\right)x^2 + \left(\frac{2N}{M}b_1 + b_2\right)xy + \frac{b_1}{M}y^2 \\ &\quad + \left(\frac{N^3}{M}b_4 + N^2b_5 + NMb_6\right)x^3 + \left(\frac{3N^2}{M}b_4 + 2Nb_5 + Mb_6\right)x^2y \\ &\quad + \left(\frac{3N}{M}b_4 + b_5\right)xy^2 + \frac{b_4}{M}y^3 + \cdots, \end{aligned}$$

$$
\begin{aligned}
g^1(x,y,s) =& f(Nx+y, Mx, s) - \frac{N}{M} g(Nx+y, Mx, s)\\
=& \left(N^2 a_1 + NMa_2 - \frac{N^3}{M} b_1 - N^2 b_2 - NMb_3\right) x^2\\
&+ \left(2Na_1 + Ma_2 - \frac{2N^2}{M} b_1 - Nb_2\right) xy + \left(a_1 - \frac{N}{M} b_1\right) y^2\\
&+ \left(N^3 a_3 + N^2 Ma_4 - \frac{N^4}{M} b_4 - N^3 b_5 - N^2 Mb_6\right) x^3\\
&+ \left(3N^2 a_3 + 2NMa_4 - \frac{3N^3}{M} b_4 - 2N^2 b_5 - NMb_6\right) x^2 y\\
&+ \left(3Na_3 + Ma_4 - \frac{3N^2}{M} b_4 - Nb_5\right) xy^2 + \left(a_3 - \frac{N}{M} b_4\right) y^3 + \cdots.
\end{aligned}
$$

Rewrite (2.9) in the following polar coordinate form:

$$
\begin{aligned}
\dot{\tau} &= \alpha(s)\tau + a(s)\tau^3 + \cdots,\\
\dot{\theta} &= \beta(s)\tau + c(s)\tau^2 + \cdots,
\end{aligned}
\tag{2.10}
$$

then the Taylor expansion of (2.10) at $s = s_0$ yields

$$
\begin{aligned}
\dot{\tau} &= \alpha'(s_0)(s-s_0)\tau + a(s_0)\tau^3 + o((s-s_0)^2\tau, (s-s_0)\tau^3, \tau^5),\\
\dot{\theta} &= \beta(s)\tau + \beta'(s_0)(s-s_0) + c(s_0)\tau^2 + o((s-s_0)^2, (s-s_0)\tau^2, \tau^4).
\end{aligned}
\tag{2.11}
$$

In order to determine the stability of the Hopf bifurcation periodic solution, we need to calculate the sign of the coefficient $a(s_0)$, which is given by

$$
a(s_0) := \frac{1}{16}(f^1_{xxx} + f^1_{xyy} + g^1_{xxy} + g^1_{yyy}) + \frac{1}{16\beta_0}[f^1_{xy}(f^1_{xx} + f^1_{yy}) - g^1_{xy}(g^1_{xx} + g^1_{yy}) - f^1_{xx} g^1_{xx} + f^1_{yy} g^1_{yy}],
$$

where all partial derivatives are evaluated at the bifurcation point $(x, y, s) = (0, 0, s_0)$ and

$$
\begin{aligned}
f^1_{xxx}(0,0,s_0) &= 6\left(\frac{N_0^3}{M_0} b_4 + N_0^2 b_5 + N_0 M_0 b_6\right),\\
f^1_{xyy}(0,0,s_0) &= 2\left(\frac{3N_0}{M_0} b_4 + b_5\right),\\
g^1_{xxy}(0,0,s_0) &= 2\left(3N_0^2 a_3 + 2N_0 M_0 a_4 - \frac{3N_0^3}{M_0} b_4 - 2N_0^2 b_5 - N_0 M_0 b_6\right),\\
g^1_{yyy}(0,0,s_0) &= 6\left(A_{30} - \frac{N_0}{M_0} b_4\right),\\
f^1_{xx}(0,0,s_0) &= 2\left(\frac{N_0^2}{M_0} b_1 + N_0 b_2 + M_0 b_3\right),
\end{aligned}
$$

$$f^1_{xy}(0,0,s_0)=\frac{2N_0}{M_0}b_1+b_2,\quad f^1_{yy}(0,0,s_0)=\frac{2}{M_0}b_1,$$
$$g^1_{xx}(0,0,s_0)=2\left(N_0^2a_1+N_0M_0a_2-\frac{N_0^3}{M_0}b_1-N_0^2b_2-N_0M_0b_3\right),$$
$$g^1_{xy}(0,0,s_0)=2N_0a_1+M_0a_2-\frac{2N_0^2}{M_0}b_1-N_0b_2,$$
$$g^1_{yy}(0,0,s_0)=2\left(a_1-\frac{N_0}{M_0}b_1\right).$$

Noting that N_0, M_0 and β_0 are defined by (2.8) and $N_0=M_0$, $b_1=b_3$, $b_5=-2b_6$, $b_2=-2b_1$, we find that $f^1_{xx}(0,0,s_0)=f^1_{xy}(0,0,s_0)=0$. Thus, we can calculate that

$$a(s_0)=\frac{1}{8}[3a_3-2b_6+N_0^2(3a_3+2a_4)]+\frac{1}{8\beta_0}\left(\frac{2b_1(a_1-b_1)}{N_0}-N_0(2a_1+a_2)[(a_1+a_2)N_0^2+a_1-b_1]\right).$$

Furthermore, from (2.8), we have

$$a(s_0)=-\frac{\sigma}{4(s_0+\sigma)^2}a_1^2+\frac{s_0}{8(s_0+\sigma)^2}a_2^2+\frac{2s_0-\sigma}{8(s_0+\sigma)^2}a_1a_2-\frac{\sigma}{4s_0(s_0+\sigma)}a_1b_1+\frac{1}{8(s_0+\sigma)}a_2b_1+\frac{1}{4s_0}b_1^2+\frac{3\sigma}{8(s_0+\sigma)}a_3-\frac{s_0}{4(s_0+\sigma)}a_4-\frac{1}{4}b_6. \tag{2.12}$$

Thus, we obtain $\mu_2=-\frac{a(s_0)}{\alpha'(s_0)}$. By Poincaré–Andronov–Hopf Bifurcation Theorem, we have the following result.

THEOREM 2.3 Assume that $a+b\geqslant ab$, (H_1) and (H_2) hold. Then system (2.1) undergoes a Hopf bifurcation at the interior equilibrium (u^*,v^*) when $s=s_0$. Furthermore,

(i) $a(s_0)$ determines the stability of the bifurcated periodic solutions: if $a(s_0)<0(>0)$; then the bifurcating periodic solutions are stable (unstable);

(ii) μ_2 determines the directions of Hopf bifurcation: if $\mu_2>0(<0)$, then the Hopf bifurcation is supercritical (subcritical).

EXAMPLE 2.4 Now we give some numerical simulations for the following particular case of system (2.1) with fixed parameters $a=3$, $b=0.1$ and $m=5$. We choose s as the bifurcation parameter.

$$\begin{cases}\dfrac{\mathrm{d}u}{\mathrm{d}t}=u(1-u)-\dfrac{5uv}{(1+3u)(1+0.1v)},\\[2mm] \dfrac{\mathrm{d}v}{\mathrm{d}t}=sv\left(1-\dfrac{v}{u}\right),\\[2mm] u(0)=0.3,\quad v(0)=0.4.\end{cases} \tag{2.13}$$

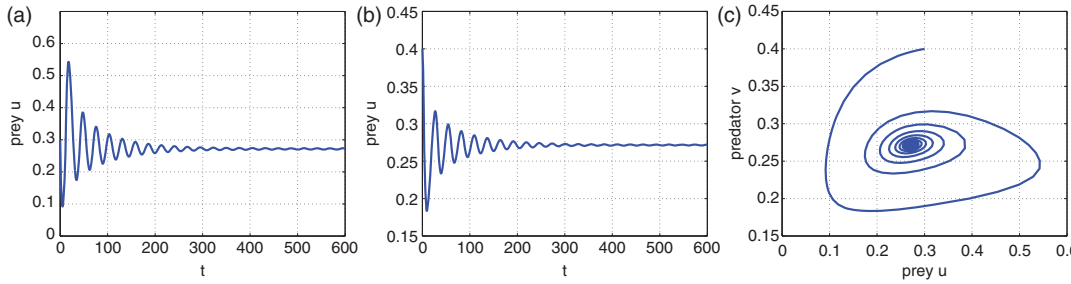

FIG. 1. When $s = 0.08 > s_0 = 0.0555$, and solutions $u(t)$ and $v(t)$ of system (2.13) converge to the equilibrium values in (a) and (b), respectively, solution trajectories spiral towards the interior equilibrium in (c).

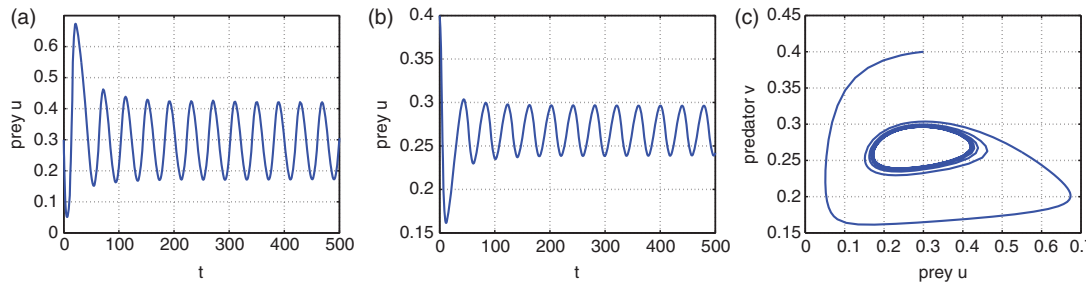

FIG. 2. When $s = 0.04 < s_0 = 0.0555$, solutions $u(t)$ and $v(t)$ of system (2.13) oscillate around the equilibrium values in (a) and (b), respectively, there is a limit cycle surrounding the interior equilibrium in (c) induced by Hopf bifurcation.

It is easy to see that $0.65 = \beta < 1 + m = 1.1$ and system (2.13) has a unique positive equilibrium $E^* = (u^*, v^*) = (0.2716, 0.2716)$. Noting that $s_0 = 0.0555$, it follows from Theorem 2.3 that E^* is locally asymptotically stable when $s > s_0 = 0.0555$ and unstable when $s < s_0 = 0.0555$. Moreover, when s passes through s_0 from the right-hand side of s_0, E^* will lose its stability and Hopf bifurcation occurs, that is, a family of periodic solutions bifurcate from the positive equilibrium. By computing, we have $a(s_0) = -0.5643$ and thus the Hopf bifurcation is subcritical and the bifurcating periodic solutions are orbitally asymptotically stable. Numerical simulations are presented in Figs 1–2. Figure 1 shows stable behaviour of the prey and predator species when $s > s_0$: In Fig. 1(a,b), both components $u(t)$ and $v(t)$ converge to their corresponding equilibrium values as time approaches infinity; in Fig. 1(c) the solution trajectories spiral towards the equilibrium point as time goes to infinity. Figure 2(a,b) present the time plots of the prey and predator species for $s < s_0$, which indicate the oscillations of the two populations induced by instability. Figure 2(c) is the phase portrait of the predator–prey model which depicts the limit cycle arising out of Hopf bifurcation around the positive equilibrium E^*.

3. Stability and bifurcations of the reaction–diffusion system

3.1 *Invariance, uniform persistence and global stability*

In this subsection, the invariance, uniform persistence and the global asymptotic stability of positive steady state (u^*, v^*) are studied for the diffusive predator–prey system (1.7). First, we will show that any non-negative solution $(u(x, t), v(x, t))$ of (1.7) lies in a certain bounded region as $t \to \infty$ for all $x \in \Omega$.

PROPOSITION 3.1 All solutions of (1.7) are non-negative. Moreover, the non-negative solution (u, v) of (1.7) satisfies

$$\limsup_{t\to\infty} \max_{\bar{\Omega}} u(\cdot, t) \leqslant 1, \quad \limsup_{t\to\infty} \max_{\bar{\Omega}} v(\cdot, t) \leqslant 1. \tag{3.1}$$

Proof. The non-negativity of solutions of (1.7) is clear since the initial values are non-negative. We only consider the boundedness.

The first inequality of (3.1) follows easily from the comparison argument for parabolic problems since

$$u(1-u) - \frac{muv}{(1+au)(1+bv)} \leqslant u(1-u), \quad (x,t) \in \Omega \times [0,\infty).$$

Thus, there exists $T \in (0,\infty)$ such that $u(x,t) \leqslant 1+\epsilon$ in $\bar{\Omega} \times [T,\infty)$ for an arbitrary $\epsilon > 0$. Since

$$sv\left(1-\frac{v}{u}\right) \leqslant sv\left(1-\frac{v}{1+\epsilon}\right) = sv\frac{(1+\epsilon)-v}{1+\epsilon}, \quad x \in \bar{\Omega}, \ \ t \geqslant T,$$

the comparison argument shows that

$$\limsup_{t\to\infty} \max_{\bar{\Omega}} v(\cdot, t) \leqslant 1+\epsilon,$$

which implies the second assertion by the arbitrariness of ϵ. The proof is completed. □

DEFINITION 3.2 System (1.7) is said to be *uniform persistent* if, for any non-negative initial data $(u_0(x), v_0(x))$ with $u_0(x) \not\equiv 0$, $v_0(x) \not\equiv 0$, there exists a positive constant $\epsilon_0 = \epsilon_0(u_0, v_0)$ such that the solution $(u(x,t), v(x,t))$ of (1.7) satisfies

$$\liminf_{t\to\infty} \min_{\bar{\Omega}} u(\cdot, t) \geqslant \epsilon_0, \quad \liminf_{t\to\infty} \min_{\bar{\Omega}} v(\cdot, t) \geqslant \epsilon_0.$$

PROPOSITION 3.3 If $m < ab$, then system (1.7) is uniformly persistent.

Proof. Noting that

$$u\left(1-u-\frac{muv}{(1+au)(1+bv)}\right) \geqslant u\left(1-u-\frac{m}{ab}\right)$$

and $m < ab$, then we have

$$\liminf_{t\to\infty} \min_{\bar{\Omega}} u(\cdot, t) \geqslant 1 - \frac{m}{ab} \triangleq K > 0. \tag{3.2}$$

Thus, for any $\epsilon\,(0 < \epsilon < K)$, there exists $T \in (0,\infty)$ such that $u(x,t) \geqslant K - \epsilon$ in $\bar{\Omega} \times [T,\infty)$. As a result, v satisfies

$$sv\left(1-\frac{v}{u}\right) \geqslant sv\left(1-\frac{v}{K-\epsilon}\right) = sv\frac{(K-\epsilon)-v}{K-\epsilon}, \quad x \in \bar{\Omega}, \ \ t \geqslant T.$$

The comparison argument concludes that

$$\liminf_{t\to\infty} \min_{\bar{\Omega}} v(\cdot, t) \geqslant K$$

by the continuity as $\epsilon \to 0$. The proof is completed. □

REMARK 3.4 By the terminology in Cantrell & Cosner (2003), Propositions 3.1 and 3.3 indeed imply that system (1.7) is permanent if $m < ab$.

For convenience, we define

$$M = 2am + m^2 + \frac{1}{4} - \frac{mK}{(1+a)(1+b)^2}. \tag{3.3}$$

THEOREM 3.5 Assume that $a + b \geqslant ab$, $m < ab$, $ma \leqslant (1 + aK)^2(1 + bK)$ and $2K > M$ (K is defined in (3.2) and M is given in (3.3)). Then the positive constant steady state (u^*, v^*) with respect to system (1.7) is globally asymptotically stable; in other words, (u^*, v^*) attracts every positive solution of (1.7).

Proof. Let $(u(x,t), v(x,t))$ be a positive solution of (1.7). Choose a Lyapunov function as follows:

$$E(t) = \int_\Omega W(u(x,t), v(x,t))\,\mathrm{d}x,$$

where

$$W(u,v) = \int \frac{u^2 - u^{*2}}{u^2}\,\mathrm{d}u + \frac{1}{s}\int \frac{v - v^*}{v}\,\mathrm{d}v.$$

Straightforward computations yield that

$$\begin{aligned}
\frac{\mathrm{d}E(t)}{\mathrm{d}t} &= \int_\Omega \{W_u(u(x,t), v(x,t))u_t + W_v(u(x,t), v(x,t))v_t\}\,\mathrm{d}x \\
&= \int_\Omega \left\{ d_1 \frac{u^2 - u^{*2}}{u^2}\Delta u + \frac{d_2}{s}\frac{v - v^*}{v}\Delta v \right\}\mathrm{d}x \\
&\quad + \int_\Omega \left\{ \frac{u^2 - u^{*2}}{u}\left(1 - u - \frac{mv}{(1+au)(1+bv)}\right) + (v - v^*)\left(1 - \frac{v}{u}\right)\right\}\mathrm{d}x \\
&= E_1(t) + E_2(t),
\end{aligned}$$

where

$$\begin{aligned}
E_1(t) &:= \int_\Omega \left\{ d_1 \frac{u^2 - u^{*2}}{u^2}\Delta u + \frac{d_2}{s}\frac{v - v^*}{v}\Delta v \right\}\mathrm{d}x \\
&= -\int_\Omega \left\{ d_1 \frac{2u^{*2}}{u^3}|\nabla u|^2 + \frac{d_2}{s}\frac{v^*}{v^2}|\nabla v|^2 \right\}\mathrm{d}x \leqslant 0
\end{aligned}$$

and

$$\begin{aligned}
E_2(t) &:= \int_\Omega \left\{ \frac{u^2 - u^{*2}}{u}\left(1 - u - \frac{mv}{(1+au)(1+bv)}\right) + (v - v^*)\left(1 - \frac{v}{u}\right)\right\}\mathrm{d}x \\
&= \int_\Omega \left\{ \frac{u^2 - u^{*2}}{u}\left[-(u - u^*) + \frac{mv^*}{(1+au^*)(1+bv^*)} - \frac{mv}{(1+au)(1+bv)}\right]\right. \\
&\quad \left. + (v - v^*)\left(\frac{v^*}{u^*} - \frac{v}{u}\right)\right\}\mathrm{d}x
\end{aligned}$$

$$
\begin{aligned}
&= \int_\Omega \left\{ \frac{u^2 - u^{*2}}{u} \left[-(u-u^*) + \frac{mav^*(1+bv)(u-u^*) - m(1+au^*)(v-v^*)}{(1+au)(1+au^*)(1+bv)(1+bv^*)} \right] \right. \\
&\quad \left. + \frac{(v-v^*)(u-u^*)}{u} - \frac{(v-v^*)^2}{u} \right\} \mathrm{d}x \\
&= -\int_\Omega \frac{1}{u} \left\{ (u-u^*)^2(u+u^*) \left[1 - \frac{mav^*}{(1+au)(1+au^*)(1+bv^*)} \right] \right. \\
&\quad \left. + \left[\frac{m(u+u^*)}{(1+au)(1+bv)(1+bv^*)} - 1 \right] (u-u^*)(v-v^*) + (v-v^*)^2 \right\} \mathrm{d}x \\
&= -\int_\Omega \frac{1}{u} \left\{ (u+u^*) \left[1 - \frac{mav^*}{(1+au)(1+au^*)(1+bv^*)} \right] \xi^2 \right. \\
&\quad \left. + \left[\frac{m(u+u^*)}{(1+au)(1+bv)(1+bv^*)} - 1 \right] \xi\eta + \eta^2 \right\} \mathrm{d}x \\
&= -\int_\Omega \begin{pmatrix} \xi & \eta \end{pmatrix} \begin{pmatrix} p(u,v) & q(u,v) \\ q(u,v) & 1 \end{pmatrix} \begin{pmatrix} \xi \\ \eta \end{pmatrix} \mathrm{d}x,
\end{aligned}
$$

in which $\xi = u - u^*$, $\eta = v - v^*$,

$$
\begin{aligned}
p(u,v) &= (u+u^*) \left[1 - \frac{mav^*}{(1+au)(1+au^*)(1+bv^*)} \right], \\
q(u,v) &= \frac{1}{2} \left[\frac{m(u+u^*)}{(1+au)(1+bv)(1+bv^*)} - 1 \right].
\end{aligned}
$$

It can be seen that $\mathrm{d}E(t)/\mathrm{d}t = E_1(t) + E_2(t) < 0$ if and only if the matrix

$$
\begin{pmatrix} p(u,v) & q(u,v) \\ q(u,v) & 1 \end{pmatrix}
$$

is positively definite, which is equivalent to $p(u,v) + 1 > 0$ and $\psi(u,v) = p(u,v) - q^2(u,v) > 0$, where

$$
\begin{aligned}
\psi(u,v) = &-\frac{1}{4} + (u+u^*) - \frac{mav^*(u+u^*)}{(1+au)(1+au^*)(1+bv^*)} \\
&- \frac{m^2(u+u^*)^2}{4(1+au)^2(1+bv)^2(1+bv^*)^2} + \frac{m(u+u^*)}{2(1+au)(1+bv)(1+bv^*)}.
\end{aligned}
$$

By the assumption that $ma \leqslant (1+aK)^2(1+bK)$, we have $p(u,v) > 0$. Furthermore, $\psi(u,v) > 0$ is fulfilled if $2K > M$, where M is given in (3.3). Hence, we can conclude that $(u(x,t), v(x,t)) \to (u^*, v^*)$ in $[L^\infty(\Omega)]^2$, which indicates that (u^*, v^*) attracts all solutions of system (1.7). Thus, the proof is completed. □

REMARK 3.6 Under different conditions we can choose another Lyapunov function

$$
W(u,v) = u - u^* - u^* \ln \frac{u}{u^*} + \frac{1}{s} \left(v - v^* - v^* \ln \frac{v}{v^*} \right).
$$

The computation process is similar to that in the proof of Theorem 3.5. This indicates that different Lyapunov functions yield different conditions guaranteeing the global stability of (u^*, v^*).

3.2 *Turing instability*

In this part, we derive conditions for the Turing instability of the spatially homogeneous equilibrium (u^*, v^*) of diffusive predator–prey system (1.7). Here we consider the special case with the no-flux boundary conditions in a 1D interval $\Omega = (0, l)$:

$$\begin{cases} \dfrac{\partial u}{\partial t} - d_1 \Delta u = u(1-u) - \dfrac{muv}{(1+au)(1+bv)}, & x \in (0,l),\ t > 0, \\ \dfrac{\partial v}{\partial t} - d_2 \Delta v = sv\left(1 - \dfrac{v}{u}\right), & x \in (0,l),\ t > 0, \\ \dfrac{\partial u}{\partial x} = \dfrac{\partial v}{\partial x} = 0, & x = 0, l,\ t > 0, \\ u(x,0) = u_0(x) \geqslant 0,\ v(x,0) = v_0(x) \geqslant 0, & x \in (0,l), \end{cases} \tag{3.4}$$

where $l > 0$ is the length of the interval. While our calculations can be carried over to higher-dimensional spatial domains, we restrict ourselves to the case of the spatial domain $(0, l)$, for which the structure of the eigenvalues is clear. To this end, let

$$\begin{pmatrix} u \\ v \end{pmatrix} = \begin{pmatrix} \rho_1 \\ \rho_2 \end{pmatrix} \exp(\lambda t + \mathrm{i}kx),$$

where λ is the growth rate of perturbation in time t, ρ_1 and ρ_2 are the amplitudes, and k is the wave number of the solutions.

The linearized system of (3.4) at (u^*, v^*) has the form

$$\begin{pmatrix} u_t \\ v_t \end{pmatrix} = L \begin{pmatrix} u \\ v \end{pmatrix} := D \begin{pmatrix} u_{xx} \\ v_{xx} \end{pmatrix} + J \begin{pmatrix} u \\ v \end{pmatrix}, \tag{3.5}$$

where J is the Jacobian matrix defined in Section 2 and $D = \operatorname{diag}(d_1, d_2)$; L is a linear operator with domain $D_L = X_C := X \oplus \mathrm{i}X = \{x_1 + \mathrm{i}x_2 : x_1, x_2 \in X\}$, where

$$X := \left\{ (u,v) \in H^2[(0,l)] \times H^2[(0,l)] \,\middle|\, \begin{array}{l} u_x(0,t) = u_x(l,t) = 0 \\ v_x(0,t) = v_x(l,t) = 0 \end{array} \right\}$$

and $H^2[(0, l)]$ denotes the standard Sobolev space. Define

$$J_k := J - k^2 D = \begin{pmatrix} s_0 - k^2 d_1 & \sigma \\ s & -s - k^2 d_2 \end{pmatrix}.$$

It is clear that the eigenvalues of the operator L are given by the eigenvalues of the matrix J_k. The characteristic equation of J_k is

$$P_k(\lambda) := \lambda^2 - \Theta(k) \cdot \lambda + \Delta(k) = 0, \tag{3.6}$$

where

$$\Theta(k) := s_0 - s - k^2(d_1 + d_2),$$
$$\Delta(k) := d_1 d_2 k^4 + (sd_1 - s_0 d_2)k^2 - s(s_0 + \sigma).$$

The roots of (3.6) yield the dispersion relation

$$\lambda_{1,2}(k) = \tfrac{1}{2}[\Theta(k) \pm \sqrt{\Theta^2(k) - 4\Delta(k)}].$$

If we assume that condition (2.4) holds, then $s_0 < 0$ and (H_1) hold. It is easy to see that $\Theta(k) < 0$ and $\Delta(k) > 0$. Thus, we can conclude that the two roots of $P_k(\lambda) = 0$ both have negative real parts for all $k \geqslant 0$. Therefore, we have the following result.

PROPOSITION 3.7 Assume that $a + b \geqslant ab$ and (2.4) hold. Then the unique positive constant steady state (u^*, v^*) of (3.4) is locally asymptotically stable.

From Proposition 2.1, we know that the interior equilibrium (u^*, v^*) of ODE model (2.1) is locally asymptotically stable when $s > s_0$. Next, we investigate the Turing stability of the spatially homogeneous equilibrium (u^*, v^*) of diffusive system (3.4) under the assumption that (H_1) and (H_2) hold. In this case, $s_0 > 0$ and $\Delta > 0$. It is well known that the coexistence equilibrium (u^*, v^*) of diffusive system (3.4) is unstable when (3.6) has at least one root with positive real part. Noting that $\Theta(k) < 0$ when $s > s_0$. Hence, (3.6) has no imaginary root with positive real part.

For the sake of convenience, define

$$\varphi(k^2) := \Delta(k) = d_1 d_2 k^4 + (sd_1 - s_0 d_2)k^2 - s(s_0 + \sigma),$$

which is a quadratic polynomial with respect to k^2. It is necessary to determine the sign of $\varphi(k^2)$. If $\varphi(k^2) < 0$, then (3.6) has two real roots in which one is positive and another is negative. When

$$G(d_1, d_2) := sd_1 - s_0 d_2 < 0, \tag{3.7}$$

it is easy to see that $\varphi(k^2)$ will take the minimum value

$$\min_k \varphi(k^2) = -s(s_0 + \sigma) - \frac{(sd_1 - s_0 d_2)^2}{4d_1 d_2} < 0 \tag{3.8}$$

at $k^2 = k^2_{\min}$, where

$$k^2_{\min} = -\frac{sd_1 - s_0 d_2}{2d_1 d_2}.$$

Define the ratio $\theta = d_2/d_1$ and let

$$\Lambda(d_1, d_2) := (sd_1 - s_0 d_2)^2 + 4s(s_0 + \sigma)d_1 d_2 = s_0^2 d_2^2 + 2s(s_0 + 2\sigma)d_1 d_2 + s^2 d_1^2.$$

Then

$$\Lambda(d_1, d_2) = 0 \Leftrightarrow r_0^2\theta^2 + 2s(s_0 + 2\sigma)\theta + s^2 = 0,$$
$$G(d_1, d_2) = 0 \Leftrightarrow \theta = \frac{s}{s_0} \equiv \theta^*.$$

Note that $\Delta = -s(s_0 + \sigma) > 0$ and $\sigma < 0$; we have

$$4s^2(s_0 + 2\sigma)^2 - 4s^2 s_0^2 = 16s^2\sigma(s_0 + \sigma) > 0.$$

Then $\Lambda(d_1, d_2) = 0$ has two positive real roots

$$\theta_1 = \frac{-s(s_0 + 2\sigma) + 2s\sqrt{\sigma(s_0 + \sigma)}}{s_0^2}, \tag{3.9}$$

$$\theta_2 = \frac{-s(s_0 + 2\sigma) - 2s\sqrt{\sigma(s_0 + \sigma)}}{s_0^2}. \tag{3.10}$$

We can see that $0 < \theta_2 < \theta^* < \theta_1$. Therefore, when $d_2/d_1 > \theta_1$, we have $\min_k \varphi(k^2) < 0$ and $G(d_1, d_2) < 0$, and thus (u^*, v^*) is unstable. This indicates that the Turing instability occurs.

Based on the above argument, we have the following result about diffusion-driven instability.

THEOREM 3.8 Assume that $a + b \geqslant ab$, $s > s_0$, (H_1) and (H_2) hold (so the coexistence equilibrium is stable for local system (2.1)). Then there exists an unbounded region

$$U := \{(d_1, d_2) : d_1 > 0, d_2 > 0, d_2 > \theta_1 d_1\}$$

for $\theta_1 > 0$, such that, for any $(d_1, d_2) \in U$, (u^*, v^*) is unstable with respect to the reaction–diffusion system (3.4), that is, Turing instability occurs.

REMARK 3.9 We can see that $d_2/d_1 > 1$ under the assumption that $s > s_0$. Hence, for the occurrence of diffusive instability in system (3.4), the predators must diffuse faster than the prey.

EXAMPLE 3.10 As an example we consider a diffusive system with no-flux boundary conditions on 1D spatial domain $(0, l)$ and choose s as the parameter, where d_1 and d_2 are the diffusion coefficients:

$$\begin{cases} \dfrac{\partial u}{\partial t} - d_1\Delta u = u(1-u) - \dfrac{5uv}{(1+3u)(1+0.1v)}, & x \in (0,l),\ t > 0, \\ \dfrac{\partial v}{\partial t} - d_2\Delta v = sv\left(1 - \dfrac{v}{u}\right), & x \in (0,l),\ t > 0, \\ \dfrac{\partial u}{\partial v} = \dfrac{\partial v}{\partial v} = 0, & x = 0, l,\ t > 0, \\ u(x,0) = u_0(x) \geqslant 0,\ v(x,0) = v_0(x) \geqslant 0, & x \in (0,l). \end{cases} \tag{3.11}$$

Thus, when $s = 0.08 > s_0 = 0.0555$, we have $\theta_1 = (-s(s_0 + 2\sigma) + 2s\sqrt{\sigma(s_0 + \sigma)})/s_0^2 = 70.7649$. In this case, the positive equilibrium E^* of the ODE model (2.13) is stable (see Example 2.4 and Fig. 1). Now if $d_2/d_1 < \theta_1$, by Proposition 3.7 the spatially homogeneous equilibrium E^* of the diffusive system (3.11) is locally asymptotically stable. Figure 3 shows that the solutions $u(x,t)$ and $v(x,t)$ of the reaction–diffusion model (3.11) are homogeneous in the space variable and converge to the spatially homogeneous steady states u^* and v^* as the time variable increases.

To have Turing instability, with $a = 3$, $b = 0.1$, $m = 5$ and $s = 0.06$, we obtain the unstable region which is between the line $d_2 = \theta_1 d_1$ and the d_2-axis (see Fig. 5).

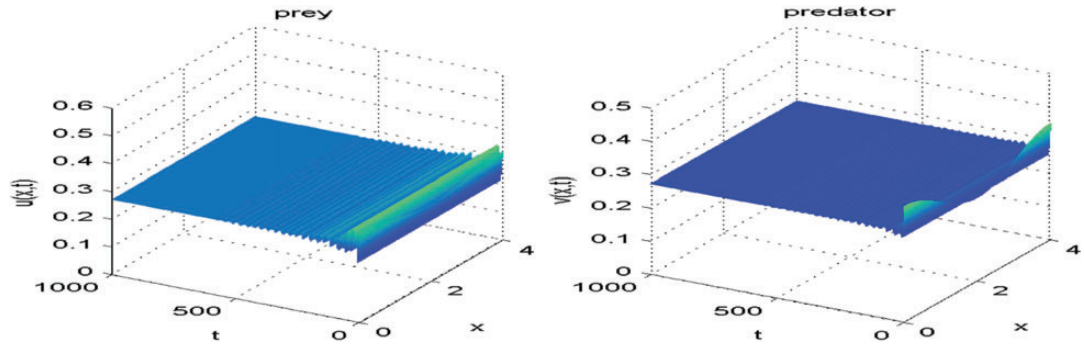

FIG. 3. Numerical simulations of the stable coexistence equilibrium solution $(u(x,t), v(x,t)$ of the reaction–diffusion system (3.11) with $s = 0.08 > s_0 = 0.0555$, $l = 4$, $d_1 = 1$, $d_2 = 1$ and $(u_0, v_0) = (0.3 + 0.02\cos(2\pi x/4), 0.3 + 0.05\cos(2\pi x/4))$, in which both $u(x,t)$ and $v(x,t)$ are homogeneous in space and converge to the spatially homogeneous steady state as time increases.

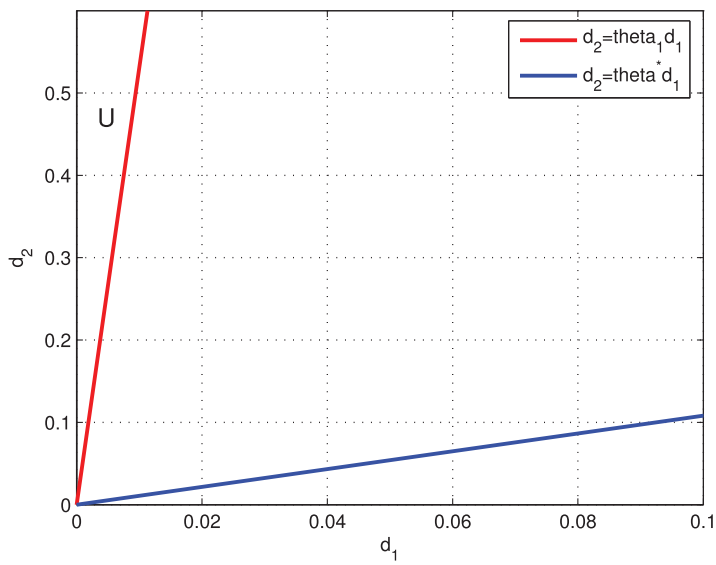

FIG. 4. Bifurcation diagram for Turing instability in the reaction–diffusion system (3.4) with $a = 3$, $b = 0.1$, $m = 5$ and $s = 0.06$. The unstable region is the area between the line $d_2 = \theta_1 d_1$ and the d_2-axis.

Therefore, according to Theorem 3.8, we know that E^* becomes unstable when $s > s_0$ and $d_2/d_1 > \theta_1 = 70.7649$, Turing instability occurs in the diffusive system (3.11), that is, both components $u^*(x,t)$ and $v^*(x,t)$ become unstable and spatially inhomogeneous (see Fig. 5).

REMARK 3.11 The Hopf bifurcation in the ODE system (2.1) gives rise to periodic solutions as stated in Theorem 2.3. Note that any periodic solution of the ODE model (2.1) is a spatially homogeneous periodic solution of the reaction–diffusion system (3.4). Follow the technique in Ruan (1998), we can show that Turing instability may occur at the stable periodic solutions of the ODE model (2.1) as well.

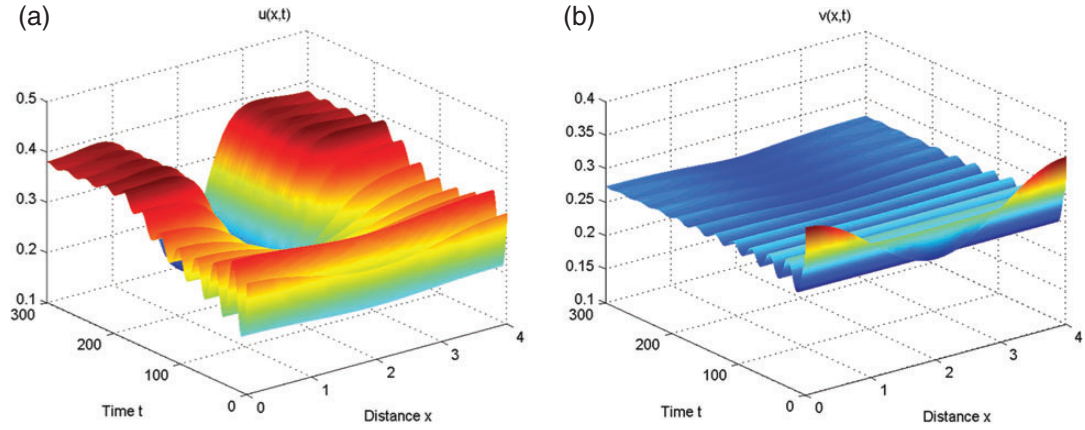

FIG. 5. Numerical simulations of Turing instability in the reaction–diffusion system (3.11) with $s = 0.08 > s_0 = 0.0555$, $l = 4$, $d_1 = 0.005$, $d_2 = 1$ and $(u_0, v_0) = (0.3 + 0.02\cos(2\pi x/4), 0.3 + 0.05\cos(2\pi x/4))$, in which both (a) $u(x,t)$ and (b) $v(x,t)$ are inhomogeneous in space and uniform in time, that is, exhibit spatial inhomogeneous patterns.

3.3 *Hopf bifurcation*

As in Theorem 2.3, we can also perform a Hopf bifurcation analysis in the diffusive system (3.4) at the same bifurcation point as in the ODE model (2.1), and bifurcating spatially homogeneous periodic solutions exist near $s = s_0$. However, due to the effect of diffusion, the stability of these periodic solutions with respect to (3.4) could be different from that for local system (2.1). Now, we shall investigate the direction of these Hopf bifurcations and stability of bifurcating periodic solutions with respect to system (3.4) by applying the normal form theory and centre manifold theorem introduced by Hassard *et al.* (1981). Let L^* be the conjugate operator of L defined as (3.5):

$$L^*\begin{pmatrix} u \\ v \end{pmatrix} := D\begin{pmatrix} u_{xx} \\ v_{xx} \end{pmatrix} + J^*\begin{pmatrix} u \\ v \end{pmatrix}, \tag{3.12}$$

where $J^* := J^\top$ with the domain $D_{L^*} = X_C$. Let

$$q := \begin{pmatrix} q_1 \\ q_2 \end{pmatrix} = \begin{pmatrix} 1 \\ -\dfrac{s_0}{\sigma} + \dfrac{\beta_0}{\sigma}\mathrm{i} \end{pmatrix}, \quad q^* := \begin{pmatrix} q_1^* \\ q_2^* \end{pmatrix} = \frac{\sigma}{2\pi\beta_0}\begin{pmatrix} \dfrac{\beta_0}{\sigma} + \dfrac{s_0}{\sigma}\mathrm{i} \\ \mathrm{i} \end{pmatrix}.$$

For any $\xi \in D_{L^*}$, $\eta \in D_L$, it is not difficult to verify that $\langle L^*\xi, \eta\rangle = \langle \xi, L\eta\rangle$, $L(s_0)q = \mathrm{i}\beta_0 q$, $L^*(s_0)q^* = -\mathrm{i}\beta_0 q^*$, $\langle q^*, q\rangle = 1$, $\langle q^*, \bar{q}\rangle = 0$, where $\langle a, b\rangle = \int_0^\pi \bar{\xi}^{\mathrm{T}}\eta \, \mathrm{d}x$ denotes the inner product in $L^2[(0,l)] \times L^2[(0,l)]$. According to Hassard *et al.* (1981), we decompose $X = X^C \oplus X^S$ with $X^C = \{zq + \bar{z}\bar{q} : z \in \mathbb{C}\}$ and $X^S = \{\omega \in X : \langle q^*, \omega\rangle = 0\}$.

For any $(u, v) \in X$, there exists $z \in \mathbb{C}$ and $\omega = (\omega_1, \omega_2) \in X^S$ such that

$$(u, v)^\top = zq + \bar{z}\bar{q} + (\omega_1, \omega_2)^\top, \quad z = \langle q^*, (u, v)^\top\rangle.$$

Thus,

$$\begin{cases} u = z + \bar{z} + \omega_1, \\ v = z\left(\dfrac{-s_0}{\sigma} + \mathrm{i}\dfrac{\beta_0}{\sigma}\right) + \bar{z}\left(\dfrac{-s_0}{\sigma} - \mathrm{i}\dfrac{\beta_0}{\sigma}\right) + \omega_2. \end{cases}$$

System (3.4) is reduced to the following system in (z, ω) coordinates:

$$\begin{cases} \dfrac{\mathrm{d}z}{\mathrm{d}t} = \mathrm{i}\beta_0 z + \langle q^*, \tilde{h}\rangle, \\ \dfrac{\mathrm{d}\omega}{\mathrm{d}t} = L\omega + H(z, \bar{z}, \omega), \end{cases} \tag{3.13}$$

where

$$H(z, \bar{z}, \omega) = \tilde{h} - \langle q^*, \tilde{h}\rangle q - \langle \bar{q}^*, \tilde{h}\rangle \bar{q}$$

and $\tilde{h} = (f, g)^\top$ (f and g are defined in (2.7)).

It is easy to obtain that

$$\begin{aligned} \langle q^*, \tilde{h}\rangle &= \frac{1}{2\beta_0}[\beta_0 f - \mathrm{i}(s_0 f + \sigma g)], \\ \langle \bar{q}^*, \tilde{h}\rangle &= \frac{1}{2\beta_0}[\beta_0 f + \mathrm{i}(s_0 f + \sigma g)], \\ \langle q^*, \tilde{h}\rangle q &= \frac{1}{2\beta_0}\begin{pmatrix} \beta_0 f - \mathrm{i}(s_0 f + \sigma g) \\ \beta_0 g + \mathrm{i}\left(\dfrac{\beta_0^2}{\sigma} f + \dfrac{\frac{s_0^2}{\sigma} f + s_0 g}{}\right) \end{pmatrix}, \\ \langle \bar{q}^*, \tilde{h}\rangle \bar{q} &= \frac{1}{2\beta_0}\begin{pmatrix} \beta_0 f + \mathrm{i}(s_0 f + \sigma g) \\ \beta_0 g - \mathrm{i}\left(\dfrac{\beta_0^2}{\sigma} f + \dfrac{s_0^2}{\sigma} f + s_0 g\right) \end{pmatrix}. \end{aligned}$$

Furthermore, we can get $H(z, \bar{z}, \omega) = (0, 0)^\top$. Let

$$H = \frac{H_{20}}{2} z^2 + H_{11} z\bar{z} + \frac{H_{02}}{2}\bar{z}^2 + o(|z|^3).$$

It follows from Appendix A of Hassard *et al.* (1981) that the system (3.13) possesses a centre manifold, and then we can write ω in the form

$$\omega = \frac{\omega_{20}}{2} z^2 + \omega_{11} z\bar{z} + \frac{\omega_{02}}{2}\bar{z}^2 + o(|z|^3).$$

Thus, we have

$$\begin{cases} \omega_{20} = (2\mathrm{i}\beta_0 I - L)^{-1} H_{20}, \\ \omega_{11} = (-L)^{-1} H_{11}, \\ \omega_{02} = \bar{\omega}_{20}. \end{cases}$$

This implies that $\omega_{20} = \omega_{02} = \omega_{11} = 0$.

For later uses, define

$$
\begin{aligned}
c_0 &:= f_{uu}q_1^2 + 2f_{uv}q_1q_2 + f_{vv}q_2^2 = 2a_1 + 2a_2q_2,\\
d_0 &:= g_{uu}q_1^2 + 2g_{uv}q_1q_2 + g_{vv}q_2^2 = 2b_1 + 2b_2q_2 + 2b_3q_2^2,\\
e_0 &:= f^1_{uu}|q_1|^2 + f^1_{uv}(q_1\bar{q}_2 + \bar{q}_1q_2) + f^1_{vv}|q_2|^2 = 2a_1 + a_2(q_2 + \bar{q}_2),\\
f_0 &:= g_{uu}|q_1|^2 + g_{uv}(q_1\bar{q}_2 + \bar{q}_1q_2) + g_{vv}|q_2|^2\\
&= 2b_1 + b_2(q_2 + \bar{q}_2) + 2b_3|q_2|^2,\\
g_0 &:= f_{uuu}|q_1|^2q_1 + f_{uuv}(2|q_1|^2q_2 + q_1^2\bar{q}_2) + f_{uvv}(2q_1|q_2|^2 + \bar{q}_1q_2^2) + f_{vvv}|q_2|^2q_2,\\
&= 6a_3 + 2a_4(2q_2 + \bar{q}_2),\\
h_0 &:= g_{uuu}|q_1|^2q_1 + g_{uuv}(2|q_1|^2q_2 + q_1^2\bar{q}_2) + g_{uvv}(2q_1|q_2|^2 + \bar{q}_1q_2^2) + g_{vvv}|q_2|^2q_2\\
&= 6b_4 + 2b_5(2q_2 + \bar{q}_2) + 2b_6(2|q_2|^2 + q_2^2),
\end{aligned}
$$

with all the partial derivatives evaluated at the point $(u, v, s) = (0, 0, s_0)$. Therefore, the reaction–diffusion system restricted to the centre manifold in $z, \bar{z}$ coordinates is given by

$$
\frac{\mathrm{d}z}{\mathrm{d}t} = \mathrm{i}\beta_0 z + \frac{1}{2}\phi_{20}z^2 + \phi_{11}z\bar{z} + \frac{1}{2}\phi_{02}\bar{z}^2 + \frac{1}{2}\phi_{21}z^2\bar{z} + o(|z|^4),
$$

where

$$
\phi_{20} = \langle q^*, (c_0, d_0)^\top\rangle, \quad \phi_{11} = \langle q^*, (e_0, f_0)^\top\rangle, \quad \phi_{21} = \langle q^*, (g_0, h_0)^\top\rangle.
$$

Note that $b_1 = b_3$, $b_2 = -2b_1$, $b_5 = -2b_6$ and $\beta_0^2 = -s_0(s_0 + \sigma)$. Then straightforward but tedious calculations show that

$$
\begin{aligned}
\phi_{20} &= \frac{\sigma}{2\beta_0}\left[\left(\frac{\beta_0}{\sigma} - \frac{s_0}{\sigma}\mathrm{i}\right)c_0 - \mathrm{i}d_0\right]\\
&= a_1 - 2b_1 - \frac{2}{\sigma}b_1s_0 - \frac{\mathrm{i}}{\beta_0}\left(\frac{2}{\sigma}b_1s_0^2 + (a_1 + a_2 + 3b_1)s_0 + \sigma b_1\right),\\
\phi_{11} &= \frac{\sigma}{2\beta_0}\left[\left(\frac{\beta_0}{\sigma} - \frac{s_0}{\sigma}\mathrm{i}\right)e_0 - \mathrm{i}f_0\right]\\
&= a_1 - \frac{1}{\sigma}a_2s_0 - \frac{\mathrm{i}}{\beta_0}\left(-\frac{1}{\sigma}a_2s_0^2 + (a_1 + b_1)s_0 + \sigma b_1\right),\\
\phi_{21} &= \frac{\sigma}{2\beta_0}\left[\left(\frac{\beta_0}{\sigma} - \frac{s_0}{\sigma}\mathrm{i}\right)g_0 - \mathrm{i}h_0\right]\\
&= 3a_3 - 2b_6 - \frac{2}{\sigma}(a_4 + b_6)s_0 + \frac{\mathrm{i}}{\beta_0}\left(\frac{2}{\sigma}(a_4 - b_6)s_0^2 - (3a_3 + a_4 + 5b_6)s_0 - 3\sigma b_4\right).
\end{aligned}
$$

According to Hassard *et al.* (1981), we have

$$\begin{aligned}
\mathrm{Re}(c_1(s_0)) &= \mathrm{Re}\left\{\frac{\mathrm{i}}{2\beta_0}\left(\phi_{20}\phi_{11} - 2|\phi_{11}|^2 - \frac{1}{3}|\phi_{02}|^2\right) + \frac{1}{2}\phi_{21}\right\} \\
&= -\frac{1}{2\beta_0}[\mathrm{Re}(\phi_{20})\,\mathrm{Im}(\phi_{11}) + \mathrm{Im}(\phi_{20})\,\mathrm{Re}(\phi_{11})] + \frac{1}{2}\mathrm{Re}(\phi_{21}) \\
&= -\frac{a_2^2 + 2a_1a_2 + a_2b_1 + 2b_1^2}{2\beta_0^2\sigma}s_0^2 + \frac{\sigma b_1(a_1 - b_1)}{\beta_0^2} + \frac{3}{2}a_3 - b_6 \\
&\quad + \left(\frac{2(a_1^2 + a_1b_1 - 2b_1^2) + a_2(a_1 - b_1)}{2\beta_0^2} - \frac{a_4}{\sigma} - \frac{b_6}{\sigma}\right)s_0 \\
&= -\frac{1}{s_0 + \sigma}a_1^2 + \frac{s_0}{2(s_0 + \sigma)\sigma}a_2^2 + \frac{2s_0 - \sigma}{2(s_0 + \sigma)\sigma}a_1a_2 \\
&\quad - \frac{1}{s_0}a_1b_1 + \frac{1}{2\sigma}a_2b_1 + \frac{s_0 + \sigma}{s_0\sigma}b_1^2 + \frac{3}{2}a_3 - \frac{s_0}{\sigma}a_4 - \frac{s_0 + \sigma}{\sigma}b_6. \qquad (3.14)
\end{aligned}$$

Based on the above analysis, we give our results in the following theorem.

THEOREM 3.12 Suppose that $a + b \geqslant ab$, (H_1) and (H_2) hold. Then system (3.4) undergoes Hopf bifurcation at $s = s_0$.

(i) The direction of Hopf bifurcation is subcritical and the bifurcating (spatially homogeneous) periodic solutions are orbitally asymptotically stable if $\mathrm{Re}(c_1(s_0)) < 0$.

(ii) The direction of Hopf bifurcation is supercritical and the bifurcating periodic solutions are unstable if $\mathrm{Re}(c_1(s_0)) > 0$.

REMARK 3.13 From (2.12) and (3.14), we can find that $\mathrm{Re}(c_1(s_0)) = 4(s_0 + \sigma)a(s_0)/\sigma$. Under the conditions that (H_1) and (H_2) hold, we have $s_0 + \sigma < 0$. Then $\mathrm{Re}(c_1(s_0)) < 0 (> 0)$ if and only if $a(s_0) < 0 (> 0)$ since $4(s_0 + \sigma)/\sigma > 0$. We can conclude that the direction of Hopf bifurcation of system (3.4) is the same as that of local system (2.1).

EXAMPLE 3.14 As in Example 3.10, we continue to consider the diffusive system (3.11). By Theorem 3.12, for the reaction–diffusion system (3.11) Hopf bifurcation occurs at $s = s_0$ and the bifurcating temporal periodic solutions exist when $s < s_0$. Choosing $s = 0.03 < 0.0555$, we have $\mathrm{Re}(c_1(s_0)) = -2.0806 < 0$, which indicates that the bifurcating temporal periodic solutions are orbitally asymptotically stable (see Fig. 6). Comparing with Fig. 3, we can see that the solutions $u(x, t)$ and $v(x, t)$ of the reaction–diffusion model (3.11) are homogeneous in the space variable and oscillatory in the time variable about the spatially homogeneous steady states u^* and v^*.

3.4 *Turing–Hopf bifurcation*

Ecologically speaking, the Turing instability breaks the spatial symmetry leading to the pattern formation that is stationary in time and oscillatory in space, while the Hopf bifurcation breaks the temporal symmetry of the system and gives rise to oscillations which are uniform in space and periodic in time. In this part, we will investigate the coupling between two different instabilities, i.e. Turing–Hopf bifurcation, in the (s, d_1)-parameter space.

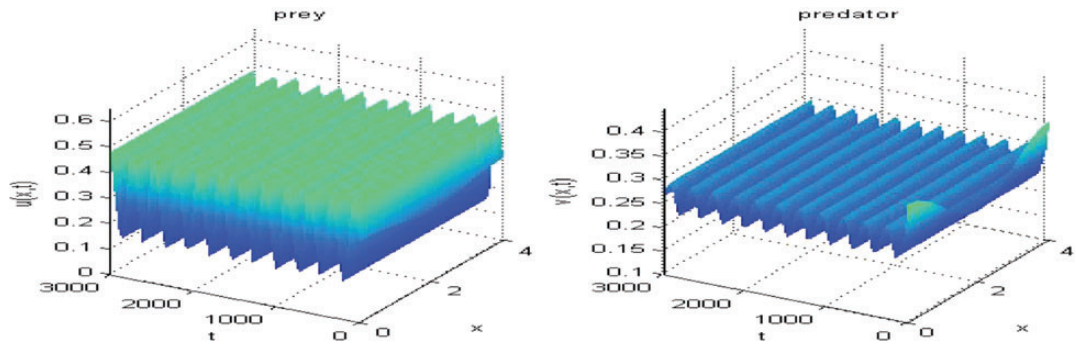

FIG. 6. Numerical simulations of the stable time-periodic solutions for the reaction–diffusion system (3.11) with $s = 0.08 > s_0 = 0.0555$, $l = 4$, $d_1 = 0.004$, $d_2 = 1$ and $(u_0, v_0) = (0.3 + 0.02\cos(2\pi x/4), 0.3 + 0.05\cos(2\pi x/4))$, in which both $u(x,t)$ and $v(x,t)$ are oscillatory in time and homogeneous in space, that is, exhibit temporal periodic patterns.

Assume that $a + b \geqslant ab$, (H_1) and (H_2) hold. We choose s as the bifurcation parameter. From Theorem 3.12, we know that the critical value of the Hopf bifurcation parameter s is

$$s^H = s_0 = u^* \left(\frac{amu^*}{(1 + au^*)^2(1 + bu^*)} - 1 \right). \tag{3.15}$$

At the bifurcation point, the frequency of these temporal oscillations is given by

$$\omega_H = \mathrm{Im}(\lambda) = \sqrt{\Delta(k = 0)} = \sqrt{-s(s_0 + \sigma)}.$$

Based on the analysis in Section 3.1, we know that the Turing instability occurs when $d_1 \ll d_2$. In the following, we fix $d_2 = 1$. From (3.9), the critical value of the Turing bifurcation parameter s takes the form

$$s^T = \frac{s_0^2}{d_1(-(s_0 + 2\sigma) + \sqrt{-\sigma(s_0 + \sigma)})}. \tag{3.16}$$

At the Turing instability threshold, the bifurcation of stationary spatially periodic patterns is characterized by the wavenumber k_T with

$$k_T = \sqrt{\frac{-s(s_0 + \sigma)}{d_1}}.$$

In Fig. 7, the Turing bifurcation curve and Hopf bifurcation curve are plotted in the (s, d_1)-parameter space for fixed $m = 5$, $a = 3$, $b = 0.1$ and $d_2 = 1$. The Hopf bifurcation and Turing bifurcation curves divide the parametric space into four distinct regions. In region I, the upper part of the displayed parameter space, the coexistence equilibrium is the only stable solution of diffusive system (3.4). Domain II is the region of pure Turing bifurcation, while domain III is the region of pure Hopf bifurcation. In domain IV, located below the two bifurcation curves, both Turing instability and Hopf bifurcation occur. This can give rise to an interaction of both types, producing particularly complex spatiotemporal patterns if the thresholds for both instabilities occur close to each other. This is the case in the neighbourhood of a degenerate point (marked by TH), where the Turing and the Hopf bifurcations coincide: this is called a codimension-2 Turing–Hopf point, since two control variables are necessary to fix these bifurcation points in a generic system of equations.

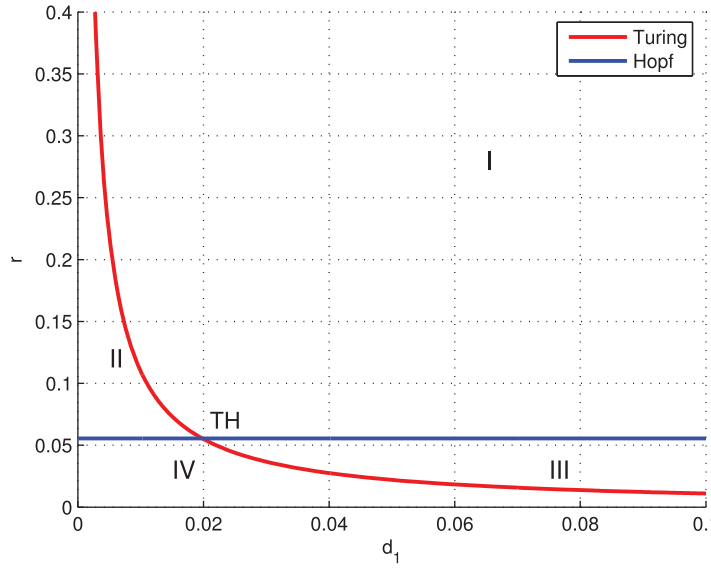

FIG. 7. Turing–Hopf bifurcation diagram for the reaction–diffusion system (3.4) with $m = 5$, $a = 3$, $b = 0.1$ and $d_2 = 1$.

At the Turing–Hopf point, we have $s^{\mathrm{H}} = s^{\mathrm{T}}$ (s^{H} and s^{T} are given in (3.15) and (3.16)). Thus, we can obtain the critical value of d_1:

$$d_1^* = \frac{s_0}{(\sqrt{-\sigma} + \sqrt{-(s_0 + \sigma)})^2}.$$

REMARK 3.15 If $d_1 < d_1^*$, then $s^{\mathrm{H}} < s^{\mathrm{T}}$. With increasing s, the Hopf threshold is the first to be crossed and thus Hopf bifurcation will be the first to occur near the criticality. On the contrary, if $d_1 > d_1^*$, the first bifurcation will occur towards Turing patterns.

EXAMPLE 3.16 As in Examples 3.10 and 3.14, we still consider the reaction–diffusion system (3.11). From Section 3.3, we know that when (s, d_1) is in region IV, the interaction of Turing instability and Hopf bifurcation occurs. Figure 8 shows the Turing–Hopf structures for the diffusive system (3.11). Moreover, in order to observe the spatiotemporal patterns of Turing–Hopf bifurcation in a 2D spatial domain when the parameters locate in region IV in Fig. 7, we should discretize the space and the time of the problem because the dynamical behaviour of the spatial predator–prey system cannot be investigated by using analytical methods or normal forms. We will transform it from an infinite-dimensional (continuous) to a finite-dimensional (discrete) form. In practice, the continuous problem defined by the reaction–diffusion system in a 2D space domain is solved in a discrete domain with $M \times N$ lattice sites. The spacing between the lattice points is defined by the lattice constant Δh. In the discrete system, the Laplacian describing diffusion is calculated by using finite difference schemes, i.e. the derivatives are approximated by differences over Δh. For $\Delta h \to 0$, the differences approach the derivatives. The time evolution is also discrete, that is, the time goes by steps of Δt, and is solved by using the Euler method, which means approximating the value of the concentration at the next step based on the change rate of the concentration at the previous time step. The model (3.11) is solved by numerically approximating the spatial derivatives and an explicit Euler's method for the time integration with a time step $\Delta t = 0.01$ and space step size $\Delta h = 1.25$. In order to avoid numerical artefacts, we checked the sensitivity of the

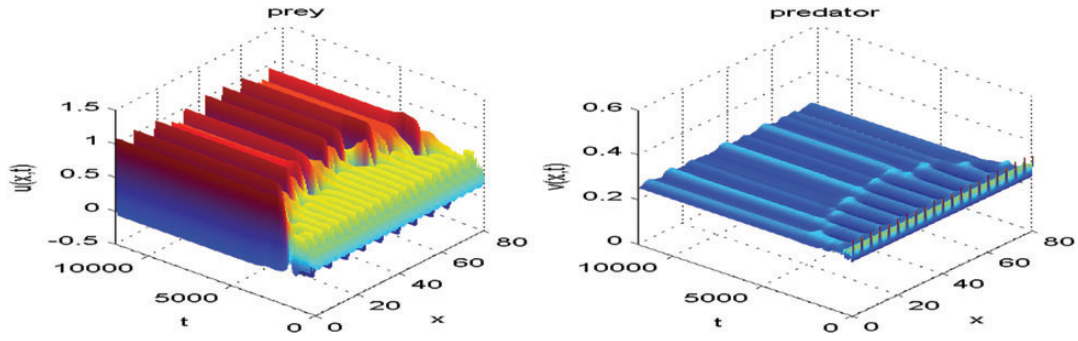

FIG. 8. Numerical simulations of Turing–Hopf structures for the reaction–diffusion system (3.11) with $s = 0.04 < s_0 = 0.0555$, $l = 80$, $d_1 = 0.001$, $d_2 = 1$ and $(u_0, v_0) = (0.3 + 0.02\cos(2\pi x/4), 0.3 + 0.05\cos(2\pi x/4))$, in which both $u(x,t)$ and $v(x,t)$ are inhomogeneous in space and non-uniform in time, that is, exhibit spatiotemporal patterns.

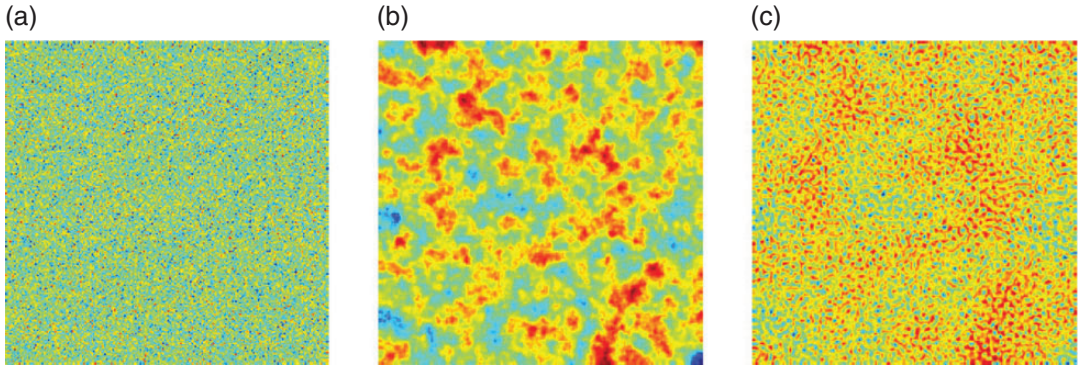

FIG. 9. Snapshots of contour pictures of the time evolution of the prey population density at different instants for the reaction–diffusion system (3.11) in a 2D spatial domain with $s = 0.04 < s_0 = 0.0555$, $d_1 = 0.008$ and $d_2 = 1$. (a) 0 iteration; (b) 2000 iterations; (c) 10000 iterations.

results to the choice of the time and space steps and their values have been chosen sufficiently small. Both numerical schemes are standard, hence we do not describe them here.

In the simulations, different types of dynamics are observed and we have found that the distributions of predators and the prey are always of the same type. So, we can restrict our analysis of pattern formation to one distribution (for instance, we show the distribution of the prey in this paper). The initial density distributions are random spatial distributions of the species, which is more general from the biological point of view. In Fig. 9, we show the evolution of the spatial pattern of the prey at 0, 2000 and 10000 iterations, with random perturbation of the steady states u^* and v^*. We see from this figure that the spotted and labyrinth patterns prevail over the whole domain.

4. Positive non-constant steady states

In this section, we use the Leray–Schauder degree theory to study the existence and non-existence of positive non-constant steady states of system (1.7), that is, the existence and non-existence of positive

non-constant solutions of the corresponding elliptic system:

$$\begin{cases} -d_1\Delta u = u(1-u) - \dfrac{muv}{(1+au)(1+bv)}, & x\in\Omega,\\ -d_2\Delta v = sv\left(1-\dfrac{v}{u}\right), & x\in\Omega,\\ \dfrac{\partial u}{\partial \nu} = \dfrac{\partial v}{\partial \nu} = 0, & x\in\partial\Omega. \end{cases} \tag{4.1}$$

Let $0=\mu_0<\mu_1<\mu_2<\cdots\to\infty$ be the eigenvalues of $-\Delta$ on Ω under homogeneous Neumann boundary condition. By $S(\mu_i)$, we denote the space of eigenfunctions corresponding to μ_i for $i=0,1,2,\ldots$. $\mathbf{X}_{ij}:=\{\mathbf{c}\cdot\varphi_{ij}:\mathbf{c}\in\mathbb{R}^2\}$, where $\{\varphi_{ij}\}$ are orthonormal basis of $S(\mu_i)$ for $j=1,2,\ldots,\dim[S(\mu_i)]$. $\mathbf{X}:=\{\mathbf{u}=(u,v)\in[C^1(\bar\Omega)]^2:\partial u/\partial\nu=\partial v/\partial\nu=0\}$, and so $\mathbf{X}=\bigoplus_{i=1}^{\infty}\mathbf{X}_i$, where $\mathbf{X}_i=\bigoplus_{j=1}^{\dim[S(\mu_i)]}\mathbf{X}_{ij}$.

4.1 *A priori estimates*

It is necessary to establish *a priori* positive upper and lower bounds for the positive solution of (4.1). We first cite two lemmas which are due to Lin *et al.* (1988) and Lou & Ni (1996).

LEMMA 4.1 (Harnack Inequality Lin *et al.*, 1988) Assume that $c\in C(\bar\Omega)$ and let $w\in C^2(\Omega)\cap C^1(\bar\Omega)$ be a positive solution to $\Delta w(x)+c(x)w(x)=0$ in Ω and $\partial w/\partial\nu=0$ on $\partial\Omega$. Then there exists a positive constant $C_*=C_*(\|c\|_\infty)$ such that

$$\max_{\bar\Omega} w \leqslant C_* \min_{\bar\Omega} w.$$

LEMMA 4.2 (Maximum Principle Lou & Ni, 1996) Suppose that $g\in C(\bar\Omega\times\mathbb{R})$.

(i) Assume that $w\in C^2(\Omega)\cap C^1(\bar\Omega)$ satisfies $\Delta w(x)+g(x,w(x))\geqslant 0$ in Ω and $\partial w/\partial\nu\leqslant 0$ on $\partial\Omega$. If $w(x_0)=\max_{\bar\Omega} w$; then $g(x_0,w(x_0))\geqslant 0$.

(ii) Assume that $w\in C^2(\Omega)\cap C^1(\bar\Omega)$ satisfies $\Delta w(x)+g(x,w(x))\leqslant 0$ in Ω and $\partial w/\partial\nu\geqslant 0$ on $\partial\Omega$. If $w(x_0)=\min_{\bar\Omega} w$; then $g(x_0,w(x_0))\leqslant 0$.

Note that the positive solutions of (4.1) are contained in $C^2(\bar\Omega)\times C^2(\bar\Omega)$ by the standard regularity theory for elliptic equations (Gilbarg & Trudinger, 2001), so Lemmas 4.1 and 4.2 can be applied to (4.1) after proper estimates. For notational convenience, we write $\Gamma=\Gamma(a,b,m,s)$ in the sequel.

THEOREM 4.3 (Upper bounds) For any positive solution (u,v) of (4.1),

$$\max_{\bar\Omega} u(x)\leqslant 1, \quad \max_{\bar\Omega} v(x)\leqslant 1. \tag{4.2}$$

Proof. A direct application of Lemma 4.2 to the first equation of (4.1) yields the first inequality of (4.2). Since $0<v\leqslant\|u\|_\infty\leqslant 1$, we have $v(x)\leqslant 1$ in $\bar\Omega$. □

THEOREM 4.4 (Lower bounds) Let d be a fixed positive constant. Then, for $d_1,d_2\geqslant d$, there exists a positive constant $\underline{C}=\underline{C}(\Gamma,d)$ such that any positive solution (u,v) of (4.1) satisfies

$$\min_{\bar\Omega} u(x)\geqslant \underline{C}, \quad \min_{\bar\Omega} v(x)\geqslant \underline{C}.$$

Proof. Let

$$u(x_0) = \min_{\bar{\Omega}} u(x), \quad v(y_0) = \min_{\bar{\Omega}} v(x), \quad v(y_1) = \max_{\bar{\Omega}} v(x).$$

By Lemma 4.2, it is clear that

$$1 - u(x_0) - \frac{mv(x_0)}{(1+au(x_0))(1+bv(x_0))} \leqslant 0, \quad 1 - \frac{v(y_0)}{u(y_0)} \leqslant 0, \quad 1 - \frac{v(y_1)}{u(y_1)} \geqslant 0,$$

and so

$$u(x_0) \leqslant u(y_0) \leqslant v(y_0), \tag{4.3}$$

$$v(y_1) \leqslant u(y_1) \leqslant \max_{\bar{\Omega}} u(x). \tag{4.4}$$

From (4.4), we have

$$1 - u(x_0) \leqslant \frac{m}{(1+au(x_0))(1+bv(x_0))} v(x_0) \leqslant mv(x_0) \leqslant m \max_{\bar{\Omega}} v(x) \leqslant m \max_{\bar{\Omega}} u(x).$$

These estimates imply that

$$1 \leqslant u(x_0) + m \max_{\bar{\Omega}} u(x) = \min_{\bar{\Omega}} u(x) + m \max_{\bar{\Omega}} u(x). \tag{4.5}$$

Define

$$c(x) = d_1^{-1} \left(1 - u - \frac{mv}{(1+au)(1+bv)} \right);$$

then u satisfies

$$\Delta u + c(x)u = 0 \ \text{ in } \Omega, \quad \frac{\partial u}{\partial \nu} = 0 \ \text{ on } \partial\Omega.$$

Lemma 4.1 further indicates that

$$\max_{\bar{\Omega}} u(x) \leqslant C_* \min_{\bar{\Omega}} u(x),$$

where C_* is a positive constant depending on $\|c\|_\infty$.

Combining this with (4.5), we obtain

$$u(x_0) = \min_{\bar{\Omega}} u(x) \geqslant \frac{1}{1+mC_*} \triangleq \underline{C}.$$

It follows from (4.3) that $v(y_0) \geqslant \underline{C}$. The proof is completed. □

4.2 *Non-existence of positive non-constant steady states*

Now we show the non-existence of positive non-constant solutions of (4.1) by the effect of large diffusivity. For convenience, we define

$$f_1(u,v) = u(1-u) - \frac{muv}{(1+au)(1+bv)} \quad \text{and} \quad f_2(u,v) = sv\left(1 - \frac{v}{u}\right). \tag{4.6}$$

THEOREM 4.5 Let $d_2^* > s/\mu_1$ be a fixed positive constant. Then there exists a positive constant $d_1^* = d_1^*(\Gamma, d_2^*)$ such that (4.1) has no positive non-constant solution provided that $d_1 \geqslant d_1^*$ and $d_2 \geqslant d_2^*$.

Proof. Assume that (u, v) is a positive solution of (4.1). Let $\bar{\varphi} = (1/|\Omega|)\int_\Omega \varphi \mathrm{d}x$ for any $\varphi \in L^1(\Omega)$. By multiplying $(u - \bar{u})$ to the first equation in (4.1) and then integrating on Ω, we have

$$\begin{aligned}\int_\Omega d_1|\nabla u|^2 \mathrm{d}x &= \int_\Omega f_1(u, v)(u - \bar{u})\,\mathrm{d}x \\ &= \int_\Omega \{f_1(u, v) - f_1(\bar{u}, \bar{v})\}(u - \bar{u})\,\mathrm{d}x \\ &= \int_\Omega \left\{[1 - (u + \bar{u})](u - \bar{u})^2 - \frac{m\bar{v}(u - \bar{u})^2}{(1 + au)(1 + a\bar{u})(1 + b\bar{v})}\right. \\ &\quad \left. - \frac{mu(u - \bar{u})(v - \bar{v})}{(1 + au)(1 + bv)(1 + b\bar{v})}\right\}\mathrm{d}x \\ &\leqslant \int_\Omega \{(u - \bar{u})^2 + m|u - \bar{u}||v - \bar{v}|\}\,\mathrm{d}x.\end{aligned}$$

Similarly, we can establish the following estimate:

$$\begin{aligned}\int_\Omega d_2|\nabla v|^2 \mathrm{d}x &= \int_\Omega f_2(u, v)(v - \bar{v})\,\mathrm{d}x \\ &= \int_\Omega \{f_2(u, v) - f_2(\bar{u}, \bar{v})\}(v - \bar{v})\,\mathrm{d}x \\ &= \int_\Omega \left\{s(v - \bar{v}) + \frac{s\bar{v}^2}{\bar{u}} - \frac{s\bar{v}^2}{u} - \frac{sv^2}{u} + \frac{s\bar{v}^2}{u}\right\}(v - \bar{v})\,\mathrm{d}x \\ &= \int_\Omega \left\{\frac{s\bar{v}^2}{u\bar{u}}(u - \bar{u})(v - \bar{v}) + \left(s - \frac{s(v + \bar{v})}{u}\right)(v - \bar{v})^2\right\}\mathrm{d}x \\ &\leqslant \int_\Omega \left\{\frac{s\bar{v}^2}{u\bar{u}}(u - \bar{u})(v - \bar{v}) + s(v - \bar{v})^2\right\}\mathrm{d}x.\end{aligned}$$

These estimates indicate that

$$\begin{aligned}\int_\Omega \{d_1|\nabla u|^2 + d_2|\nabla v|^2\}\,\mathrm{d}x &\leqslant \int_\Omega \{(u - \bar{u})^2 + 2\vartheta|u - \bar{u}||v - \bar{v}| + s(v - \bar{v})^2\}\,\mathrm{d}x \\ &\leqslant \int_\Omega \left\{(u - \bar{u})^2\left(1 + \frac{\vartheta}{\epsilon}\right) + (v - \bar{v})^2(s + \vartheta\epsilon)\right\}\mathrm{d}x\end{aligned}$$

for some positive constant ϑ and an arbitrary small positive constant ϵ, in which the last inequality follows from the following fact:

$$2\vartheta|u - \bar{u}||v - \bar{v}| = 2\sqrt{\frac{\vartheta}{\epsilon}}|u - \bar{u}| \cdot \sqrt{\vartheta\epsilon}|v - \bar{v}| \leqslant \frac{\vartheta}{\epsilon}|u - \bar{u}|^2 + \vartheta\epsilon|v - \bar{v}|^2.$$

By using the Poincáre inequality, we obtain

$$\int_\Omega \{d_1\mu_1|u - \bar{u}|^2 + d_2\mu_1|v - \bar{v}|^2\}\,\mathrm{d}x \leqslant \int_\Omega \left\{(u - \bar{u})^2\left(1 + \frac{\vartheta}{\epsilon}\right) + (v - \bar{v})^2(s + \vartheta\epsilon)\right\}\mathrm{d}x.$$

Since $d_2\mu_1 > s$, from the assumption, we can find a sufficiently small $\epsilon_0 > 0$ such that $d_2\mu_1 \geqslant s + \vartheta\epsilon_0$. Finally, by taking $d_1^* := (1/\mu_1)(1 + \vartheta/\epsilon_0)$, we can conclude that $u = \bar{u}$ and $v = \bar{v}$. This completes the proof. □

4.3 *Existence of positive non-constant steady states*

In this part, we discuss the existence of positive non-constant solutions to (4.1) when the diffusion coefficients d_1 and d_2 vary while the parameters a, k, m, δ and β are kept fixed by using the Leray–Schauder degree theory. In view of Theorem 3.8, Turing pattern occurs when the diffusion of the predators is larger than that of the prey.

For simplicity, define $\mathbf{u} = (u, v)^\top$ and $\mathbf{F} = (f_1, f_2)^\top$ (f_1, f_2 are defined in (4.6)). Thus, $\mathbf{F_u}(\mathbf{e}^*) = J$ (J is given by (2.3)) and the problem (4.1) can be written as follows:

$$\begin{cases} -\Delta\mathbf{u} = D^{-1}\mathbf{F}(\mathbf{u}), & x \in \Omega, \\ \dfrac{\partial \mathbf{u}}{\partial \nu} = 0, & x \in \partial\Omega, \end{cases} \tag{4.7}$$

where $D = \mathrm{diag}(d_1, d_2)$. Therefore, $\mathbf{u}^*$ solves (4.7) if and only if it satisfies

$$\hat{f}(d_1, d_2; \mathbf{u}) := \mathbf{u} - (I - \Delta)^{-1}\{D^{-1}\mathbf{F}(\mathbf{u}) + \mathbf{u}\} = 0 \quad \text{on} \quad \mathbf{X}, \tag{4.8}$$

where $(I - \Delta)^{-1}$ represents the inverse of $I - \Delta$ with homogeneous Neumann boundary condition. A straightforward computation reveals

$$D_{\mathbf{u}}\hat{f}(d_1, d_2; \mathbf{u}) = I - (I - \Delta)^{-1}(D^{-1}J + I).$$

For each $\mathbf{X}_i$, λ is an eigenvalue of $D_{\mathbf{u}}\hat{f}(d_1, d_2; \mathbf{u})$ on $\mathbf{X}_i$ if and only if $\lambda(1 + \mu_i)$ is an eigenvalue of the following matrix:

$$M_i := \mu_i I - D^{-1}J = \begin{pmatrix} \mu_i - d_1^{-1}s_0 & -d_1^{-1}\sigma \\ -d_2^{-1}s & \mu_i + d_2^{-1}s \end{pmatrix}.$$

Clearly,

$$\det M_i = d_1^{-1}d_2^{-1}[d_1d_2\mu_i^2 + (d_1s - d_2s_0)\mu_i - s(s_0 + \sigma)]$$

and $\mathrm{tr}M_i = 2\mu_i + d_2^{-1}s - d_1^{-1}s_0$. Define

$$\hat{g}(d_1, d_2; \mu) = d_1d_2\mu^2 + (d_1s - d_2s_0)\mu - s(s_0 + \sigma).$$

Thus, $\hat{g}(d_1, d_2; \mu_i) = d_1d_2\det M_i$. If

$$(d_1s - d_2s_0)^2 > -4d_1d_2s(s_0 + \sigma), \tag{4.9}$$

then $\hat{g}(d_1, d_2; \lambda) = 0$ has two real roots, that is,

$$\mu_+(d_1, d_2) = \frac{d_2s_0 - d_1s + \sqrt{(d_2s_0 - d_1s)^2 + 4d_1d_2s(s_0 + \sigma)}}{2d_1d_2},$$

$$\mu_-(d_1, d_2) = \frac{d_2s_0 - d_1s - \sqrt{(d_2s_0 - d_1s)^2 + 4d_1d_2s(s_0 + \sigma)}}{2d_1d_2}.$$

Define

$$\mathcal{A} = \mathcal{A}(d_1, d_2) = \{\mu : \mu \geqslant 0, \mu_-(d_1, d_2) < \mu < \mu_+(d_1, d_2)\},$$
$$S_p = \{\mu_0, \mu_1, \mu_2, \ldots\},$$

and let $m(\mu_i)$ be the multiplicity of μ_i. In order to calculate the index of $\hat{f}(d_1, d_2; \cdot)$ at $\mathbf{e}^*$, we need the following lemma.

LEMMA 4.6 (Pang & Wang, 2003) Suppose $\hat{g}(d_1, d_2; \mu_i) \neq 0$ for all $\mu_i \in S_p$. Then

$$\operatorname{index}(\hat{f}(d_1, d_2; \cdot), \mathbf{e}^*) = (-1)^\sigma,$$

where

$$\sigma = \begin{cases} \displaystyle\sum_{\mu_i \in \mathcal{A} \cap S_p} m(\mu_i) & \text{if } \mathcal{A} \cap S_p \neq \emptyset, \\ 0 & \text{if } \mathcal{A} \cap S_p = \emptyset. \end{cases}$$

In particular, if $\hat{g}(d_1, d_2; \mu_i) > 0$ for all $\mu_i \geqslant 0$, then $\sigma = 0$.

From Lemma 4.6, in order to calculate the index of $\hat{f}(d_1, d_2; \cdot)$ at $\mathbf{e}^*$, we need to determine the range of μ for which $\hat{g}(d_1, d_2; \mu) < 0$.

THEOREM 4.7 Suppose that $a + b \geqslant ab$ and (H_2) hold. If $s_0/d_1 \in (\mu_k, \mu_{k+1})$ for some $k \geqslant 1$, and $\sigma_k = \Sigma_{i=1}^k m(\mu_i)$ is odd, then there exists a positive constant d^*, such that system (4.1) has at least one positive non-constant solution for all $d_2 \geqslant d^*$.

Proof. Since (H_2) holds, equivalently, $s_0 > 0$, it follows that if d_2 is large enough, then (4.9) holds and $\mu_+(d_1, d_2) > \mu_-(d_1, d_2) > 0$. Furthermore,

$$\lim_{d_2 \to \infty} \mu_+(d_1, d_2) = \frac{s_0}{d_1}, \quad \lim_{d_2 \to \infty} \mu_-(d_1, d_2) = 0.$$

As $s_0/d_1 \in (\mu_k, \mu_{k+1})$, there exists $d_0 \gg 1$ such that

$$\lambda_+(d_1, d_2) \in (\mu_k, \mu_{k+1}), \quad 0 < \mu_-(d_1, d_2) < \mu_1 \ \ \forall d_2 \geqslant d_0. \tag{4.10}$$

From Theorem 4.5, we know that there exists $d > d_0$ such that (4.1) with $d_1 = d$ and $d_2 \geqslant d$ has no positive non-constant solution. Let $d > 0$ be large enough such that $s_0/d_1 < \mu_1$; then there exists $d^* > d$ such that

$$0 < \mu_-(d_1, d_2) < \mu_+(d_1, d_2) < \lambda_1 \quad \forall d_2 \geqslant d^*. \tag{4.11}$$

Now we prove that, for any $d_2 \geqslant d^*$, (4.1) has at least one positive non-constant solution. By way of contradiction, assume that the assertion is not true for some $d_2^* \geqslant d^*$. By using the homotopy argument, we can derive a contradiction in the sequel.

Fixing $d_2 = d_2^*$, for $t \in [0,1]$, we define

$$D(t) = \begin{pmatrix} td_1 + (1-t)d & 0 \\ 0 & td_2 + (1-t)d^* \end{pmatrix}$$

and consider the following problem:

$$\begin{cases} -\Delta \mathbf{u} = D^{-1}(t)\mathbf{F}(\mathbf{u}), & x \in \Omega, \\ \dfrac{\partial \mathbf{u}}{\partial \nu} = 0, & x \in \partial\Omega. \end{cases} \tag{4.12}$$

Thus, $\mathbf{u}$ is a positive non-constant solution of (4.1) if and only if it solves (4.12) with $t = 1$. Evidently, $\mathbf{e}^*$ is the unique positive constant solution of (4.12). For any $t \in [0,1]$, $\mathbf{u}$ is a positive non-constant solution of (4.12) if and only if it is a solution of the following problem:

$$h(\mathbf{u}; t) = \mathbf{u} - (I - \Delta)^{-1}\{D^{-1}(t)\mathbf{F}(\mathbf{u}) + \mathbf{u}\} = 0, \quad \text{on } \mathbf{X}. \tag{4.13}$$

From the discussion above, we know that (4.13) has no positive non-constant solution when $t = 0$, and we have assumed that there is no such solution for $t = 1$ at $d_2 = d_2^*$. Clearly, $h(\mathbf{u}; 1) = \hat{f}(d_1, d_2; \mathbf{u})$, $h(\mathbf{u}; 0) = \hat{f}(d, d^*; \mathbf{u})$ and

$$D_u f(d_1, d_2; \mathbf{e}^*) = I - (I - \Delta)^{-1}(D^{-1}J + I),$$
$$D_u f(d, d^*; \mathbf{e}^*) = I - (I - \Delta)^{-1}(\widetilde{D}^{-1}J + I).$$

Here, $\hat{f}(\cdot, \cdot; \cdot)$ is as given in (4.8) and $\widetilde{D} = \operatorname{diag}(d, d^*)$. From (4.10) and (4.11), we have $\mathcal{A}(d_1, d_2) \cap S_p = \{\mu_1, \mu_2, \ldots, \mu_k\}$ and $\mathcal{A}(d, d^*) \cap S_p = \emptyset$. Since σ_k is odd, Lemma 4.6 yields

$$\operatorname{index}(h(\cdot; 1), \mathbf{e}^*) = \operatorname{index}(\hat{f}(d_1, d_2; \cdot), \mathbf{e}^*) = (-1)^{\sigma_q} = -1,$$
$$\operatorname{index}(h(\cdot; 0), \mathbf{e}^*) = \operatorname{index}(\hat{f}(d, d^*; \cdot), \mathbf{e}^*) = (-1)^0 = 1.$$

From Theorems 4.3 and 4.4, there exist positive constants $\underline{C} = \underline{C}(d, d_1, d^*, d_2^*, \Lambda)$ and $\bar{C} = \bar{C}(d, d^*, \Lambda)$ such that the positive solutions of (4.13) satisfy $\underline{C} < u(x), v(x) < \bar{C}$ on $\bar{\Omega}$ for all $t \in [0,1]$.

Define $\Sigma = \{\mathbf{u} \in \mathbf{X} : \underline{C} < u(x), v(x) < \bar{C}, x \in \bar{\Omega}\}$. Then $h(\mathbf{u}; t) \neq 0$ for all $\mathbf{u} \in \partial\Sigma$ and $t \in [0,1]$. By virtue of the homotopy invariance of the Leray–Schauder degree (Nirenberg, 2001), we have

$$\deg(h(\cdot; 0), \Sigma, 0) = \deg(h(\cdot; 1), \Sigma, 0). \tag{4.14}$$

Note that both equations $h(\mathbf{u}; 0) = 0$ and $h(\mathbf{u}; 1) = 1$ have the unique positive solution $\mathbf{e}^*$ in Σ, and we obtain

$$\deg(h(\cdot; 0), \Sigma, 0) = \operatorname{index}(h(\cdot; 0), \mathbf{e}^*) = 1,$$
$$\deg(h(\cdot; 1), \Sigma, 0) = \operatorname{index}(h(\cdot; 1), \mathbf{e}^*) = -1,$$

which contradicts (4.14). The proof is complete. □

5. Discussions

Pattern formation in ecological systems has been an important and fundamental topic in ecology. In their pioneering work, Segel & Jackson (1972) showed that spatial inhomogeneous patterns occur in predator–prey systems via Turing instability. However, their analysis indicates that the classical diffusive predator–prey models with prey-dependent functional response, such as the Holling type II function, cannot give rise to spatial structures through diffusion-driven instability unless the predators exhibit self-limiting or intraspecific competition. In studying a temperature-dependent reaction–diffusion predator–prey mite system on fruit trees, Wollkind *et al.* (1991) found that Turing instability occurs in a diffusive Leslie–Gower-type predator–prey model with Holling type II function, that is, a diffusive Holling–Tanner predator–prey system. This shows that the self-limiting or intraspecific competition effect of the predators can be relaxed if the carrying capacity of predator's environment is described by a Leslie–Gower term. Alonson *et al.* (2002) demonstrated that diffusive predator–prey models with ratio-dependent functional response can also generate patchiness in a homogeneous environment via Turing instability.

The prey-dependent functional response is derived based on the assumption that predators do not interfere with one another's activities (Cosner *et al.*, 1999), so the only competition among predators occurs in the depletion of prey. Predator-dependent functional response, include the Beddington–DeAngelis function (Cantrell & Cosner, 2001; Zhang *et al.*, 2012) and Crowley–Martin function (Skalski & Gilliam, 2001), describes mutual interference among predators, a phenomenon in which individuals from a population of more than two predators not only allocate time in searching for and processing their prey but also take time in encountering with other predators. The experimental observations of Skalski & Gilliam (2001) suggested use of the Beddington–DeAngelis functional response when the predator feeding rate becomes independent of predator density at high prey density and the Crowley–Martin functional response when the predator feeding rate is decreased by higher predator density even when prey density is high.

In this paper, we have considered a diffusive Leslie–Gower predator–prey system with a Crowley–Martin functional response under homogeneous Neumann boundary conditions. After studying the local stability and Hopf bifurcation in the corresponding ODE system and discussing the invariance, uniform persistence and global asymptotic stability of the coexistence equilibrium for the reaction–diffusion system, we provided detailed analyses on the spatial, temporal and spatiotemporal patterns in the reaction–diffusion model via four possible mechanisms. Firstly, we considered Turing (diffusion-driven) instability of the coexistence equilibrium for the reaction–diffusion system when the spatial domain is a bounded interval, which produces spatial inhomogeneous patterns. Then we studied the existence and direction of Hopf bifurcation and the stability of the bifurcating periodic solution in the reaction–diffusion system, which exhibits temporal periodic patterns. Next we investigated the interaction of the Turing instability and Hopf bifurcation in the reaction–diffusion system which demonstrates spatiotemporal patterns. Finally, we established the existence of positive non-constant steady states of a reaction–diffusion system. Our theoretical results further suggest that mutual interference between predators and the feeding strategy of predators are the determining factors in generating spatial and spatiotemporal patterns through predator–prey interaction in a homogeneous environment (Alonson *et al.*, 2002).

Since the Crowley–Martin functional response function is more general than the Beddington–DeAngelis functional response function and includes the Holling type II functional response function, we would like to mention that our results remain true for the diffusive Leslie–Gower predator–prey system with the Beddington–DeAngelis functional response and the diffusive Holling–Tanner predator–prey system.

Another important property of ecological systems is the existence of travelling wave solutions which describe how interacting species invade and establish. It would be very interesting to study the existence of travelling waves in the diffusive Leslie–Gower predator–prey systems with Crowley–Martin or Beddington–DeAngelis functional response. We leave this for future consideration.

Acknowledgement

This work was completed when the first author was visiting the University of Miami in 2013, he would like to thank the faculty and staff in the Department of Mathematics at the University of Miami for their warm hospitality. The authors would like to thank Dr Ying Su and Dr Gui-Quan Sun for their assistance on the numerical simulations.

Funding

This research was partially supported by the Universities Natural Science Foundation of Jiangsu Province (11KJB110003), National Natural Science Foundation of China (No.11228104, No.11461040, No.11401245) and National Science Foundation (DMS-1412454).

References

Alonson, D., Bartumeus, F. & Catalan, J. (2002) Mutual interference between predators can give rise to Turing spatial patterns. *Ecology*, **83**, 28–34.

Baurmanna, M., Gross, T. & Feudela, U. (2007) Instabilities in spatially extended predator–prey systems: Spatio-temporal patterns in the neighborhood of Turing–Hopf bifurcations. *J. Theoret. Biol.*, **245**, 220–229.

Beddington, J. R. (1975) Mutual interference between parasites or predators and its effect on searching efficiency. *J. Anim. Ecol.*, **44**, 331–340.

Cantrell, R. S. & Cosner, C. (2001) On the dynamics of predator–prey models with the Beddington–DeAngelis functional response. *J. Math. Anal. Appl.*, **257**, 206–222.

Cantrell, R. S. & Cosner, C. (2003) *Spatial Ecology via Reaction–Diffusion Equations*. Series in Computational and Mathematical Biology. Chichester, UK: John Wiley and Sons.

Caughley, G. (1976) Plant–herbivore systems. *Theoretical Ecology: Principles and Applications* (R. M. May ed.). Philadelphia, PA: W. B. Saunders Co., pp. 94–113.

Collings, J. B. (1997) The effects of the functional response on the behavior of a mite predator–prey interaction model. *J. Math. Biol.*, **36**, 149–168.

Cosner, C., DeAngelis, D. L., Ault, J. S. & Olson, D. B. (1999) Effects of spatial grouping on the functional response of predators. *Theor. Popul. Biol.*, **56**, 65–75.

Crowley, P. H. & Martin, E. K. (1989) Functional responses and interference within and between year classes of a dragonfly population. *J. N. Am. Benthol. Soc.*, **8**, 211–221.

DeAngelis, D. L., Goldstein, R. A. & O'Neill, R. V. (1975) A model for tropic interaction. *Ecology*, **56**, 881–892.

Du, Y. & Hsu, S.-B. (2004) A diffusive predator–prey model in heterogeneous environment. *J. Differ. Equ.*, **203**, 331–364.

Freedman, H. I. & Mathsen, R. M. (1993) Persistence in predator–prey systems with ratio-dependent predator influence. *Bull. Math. Biol.*, **55**, 817–827.

Gilbarg, D. & Trudinger, N.S. (2001) *Elliptic Partial Differential Equations of Second Order*. Berlin: Springer.

Hassard, B. D., Kazarinoff, N. D. & Wan, Y. H. (1981) *Theory and Applications of Hopf Bifurcation*. Cambridge: Cambridge University Press.

Holling, C. S. (1965) The functional response of predator to prey density and its role in mimicry and population regulation. *Mem. Entomol. Soc. Can.*, **45**, 1–60.

Hsu, S.-B. & Huang, T.-W. (1995) Global stability for a class of predator–prey systems. *SIAM J. Appl. Math.*, **55**, 763–783.

Huang, J., Ruan, S. & Song, J. (2014) Bifurcations in a predator–prey system of Leslie type with generalized Holling type III functional response. *J. Differ. Equ.*, **257**, 1721–1752.

Jost, C. (2000) Predator–prey theory: Hidden twins in ecology and microbiology. *Oikos*, **90**, 202–208.

Leslie, P. H. (1948) Some further notes on the use of matrices in population mathematics. *Biometrika*, **35**, 213–245.

Leslie, P. H. & Gower, J. C. (1960) The properties of a stochastic model for the predator–prey type of interaction between two species. *Biometrika*, **47**, 219–234.

Levin, S. A. (1974) Dispersion and population interactions. *Am. Nat.*, **108**, 207–228.

Levin, S. A. & Segel, L. A. (1976) Hypothesis for origin of planktonic patchiness. *Nature*, **259**, 659.

Levin, S. A. & Segel, L. A. (1985) Pattern generation in space and aspect. *SIAM Rev.*, **27**, 45–67.

Li, X., Jiang, W. & Shi, J. (2013) Hopf bifurcation and Turing instability in the reaction–diffusion Holling–Tanner predator–prey model. *IMA J. Appl. Math.*, **78**, 287–306.

Li, Y. & Xiao, D. (2007) Bifurcations of a predator–prey system of Holling and Leslie types. *Chaos Solitons Fractals*, **34**, 606–620.

Lin, L. S., Ni, W. M. & Takagi, I. (1988) Large amplitude stationary solutions to a chemotaxis systems. *J. Differ. Equ.*, **72**, 1–27.

Lou, Y. & Ni, W. M. (1996) Diffusion, self-diffusion and cross-diffusion. *J. Differ. Equ.*, **131**, 79–131.

Malchow, H., Petrovskii, S.V. & Venturino, E. (2008) *Spatiotemporal Patterns in Ecology and Epidemiology: Theory, Models, and Simulation*. Boca Raton: Chapman & Hall/CRC.

May, R. (1973) *Stability and Complexity in Model Ecosystems*. Princeton, NJ: Princeton University press.

Meixner, M., Wit, A. D., Bose, S. & Scholl, E. (1997) Generic spatiotemporal dynamics near codimension-two Turing–Hopf bifurcations. *Phys. Rev. E*, **55**, 6690–6697.

Murray, J. D. (1989) *Mathematical Biology*. Berlin: Springer.

Nirenberg, L. (2001) *Topics in Nonlinear Functional Analysis*. Providence, RI: American Mathematical Society.

Okubo, A. (1980) *Diffusion and Ecological Problems: Mathematical Models*. Berlin: Springer.

Pang, P. Y. H. & Wang, M. (2003) Qualitative analysis of a ratio-dependent predator–prey system with diffusion. *Proc. Roy. Soc. Edinburgh*, **133A**, 919–942.

Rovinsky, A. & Menzinger, M. (1992) Interaction of Turing and Hopf bifurcations in chemical systems. *Phys. Rev. A*, **46**, 6315–6322.

Ruan, S. (1998) Diffusion-driven instability in the Gierer–Meinhardt model of morphogenesis. *Natur. Resource Modeling*, **11**, 131–142.

Ruan, S., Wei, J. & Xiao, D. (1998) Hopf bifurcation in a reaction–diffusion predator–prey model with group defence. *Advanced Topics in Biomathematics*. Singapore: World Scientific Publishing, pp. 219–227.

Ryu, K. & Ahn, I. (2005) Positive solutions for ratio-dependent predator–prey interaction systems. *J. Differ. Equ.*, **218**, 117–135.

Segel, L. A. & Jackson, J. L. (1972) Dissipative structure: an explanation and an ecological example. *J. Theoret. Biol.*, **37**, 545–549.

Segel, L. A. & Levin, S. A. (1976) Applications of nonlinear stability theory to the study of the effects of dispersion on predator–prey interactions. *Selected Topics in Statistical Mechanics and Biophysics* (R. Piccirelli ed.). American Institute of Physics Symposium, vol. 27, pp. 123–152.

Skalski, G. T. & Gilliam, J. F. (2001) Functional response with predator interference: viable alternatives to the Holling Type II model. *Ecology*, **82**, 3083–3092.

Tanner, J. T. (1975) The stability and intrinsic growth rates of prey and predator populations. *Ecology*, **56**, 855–867.

Turing, A. (1952) The chemical basis of morphogenesis. *Phiol. Trans. R. Soc. Lond. Ser. B*, **237**, 37–72.

Wit, A. D., Lima, D., Dewel, G. & Borckmans, P. (1996) Spatiotemporal dynamics near a codimension-two point. *Phys. Rev. E*, **54**, 261–271.

Wollkind, J. D., Collings, J. B. & Barba, M. C. B. (1991) Diffusive instabilities in a one-dimensional temperature-dependent model system for a mite predator–prey interaction on fruit trees: Dispersal motility and aggregative preytaxis effects. *J. Math. Biol.*, **29**, 339–362.

Wollkind, J. D., Collings, J. B. & Logan, J. A. (1988) Metastability in a temperature-dependent model system for predator–prey mite outbreak interactions on fruit trees. *Bull. Math. Biol.*, **50**, 379–409.

Yi, F., Wei, J. & Shi, J. (2009) Bifurcation and spatiotemporal patterns in a homogeneous diffusive predator–prey system. *J. Differ. Equ.*, **246**, 1944–1977.

Zhang, J.-F., Li, W.-T. & Wang, Y.-X. (2011) Turing patterns of a strongly coupled predator–prey system with diffusion effects. *Nonlinear Anal.*, **74**, 847–858.

Zhang, X.-C., Sun, G.-Q. & Jin, Z. (2012) Spatial dynamics in a predator–prey model with Beddington–DeAngelis functional response. *Phys. Rev. E*, **85**, 021924.1-14.